

Contents

Materials and methods	2
<i>General methods</i>	2
<i>Optical spectroscopy</i>	3
<i>Enzyme kinetics</i>	3
<i>Cloning</i>	3
<i>Cell culture</i>	4
<i>Cell viability assays</i>	4
<i>Confocal fluorescence microscopy</i>	5
<i>Co-localization experiments</i>	6
<i>LC-MS analysis</i>	7
<i>Mitochondrial glutathione redox states in live cells</i>	8
<i>Labeling of free nucleophilic thiols in proteomes of treated cells</i>	8
<i>Superoxide production and BSO experiment</i>	9
<i>Quantitative image analysis of cell morphologies and mitochondrial/cytosolic ratios</i>	10
<i>Total RNA isolation</i>	10
<i>mRNA library preparation for sequencing</i>	11
<i>Cluster generation and sequencing</i>	11
<i>Bioinformatic analysis</i>	11
Probes Properties	12
<i>Spectroscopic Properties</i>	12
<i>Kinetic Properties</i>	14
Live Cells and Lysates	15
<i>Co-localization analysis</i>	15
<i>Fluorescence Intensities</i>	16
<i>Intracellular Concentration</i>	17
<i>Cell Viability Assays</i>	18
<i>Mitochondrial redox state: small molecule sensor</i>	19
<i>Mitochondrial redox state: roGFP2 sensor</i>	18
<i>Superoxide Production</i>	22
<i>Labeling of Free Thiols in the Proteome</i>	23
<i>Mitochondrial Morphology</i>	24
<i>Mitochondrial Morphology tmTCEP</i>	25
Plasmid Maps	26
Transcriptomic Analysis	28

<i>Enrichment Analysis</i>	28
<i>Adapter Sequences for RNA Sequencing</i>	29
Quantitative Image Analysis	32
<i>Mitochondrial Morphologies</i>	32
<i>Membrane Depolarization</i>	34
<i>Co-localization of LC3 punctae and Mitochondria</i>	35
Probe Characterization	39
<i>Synthesis of Probes</i>	39
<i>NMR Spectra</i>	44
Bibliography	52

Materials and methods

General methods

All reagents were purchased from commercial sources and used without further purification. Solvents were obtained from Sigma-Aldrich and used as received. NMR spectra were acquired on a Bruker AV300 or Bruker 400 instruments. ^1H NMR chemical shifts are reported in ppm relative to SiMe_4 ($\delta = 0$) and were referenced internally with respect to residual protons in the solvent ($\delta = 1.94$ for CD_3CN , $\delta = 3.31$ for CD_3OD and $\delta = 2.50$ for DMSO-d_6). Coupling constants are reported in Hz. ^{13}C NMR chemical shifts are reported in ppm relative to SiMe_4 ($\delta = 0$) and were referenced internally with respect to solvent signal ($\delta = 118.3$ for CD_3CN , $\delta = 49.0$ for CD_3OD and $\delta = 39.5$ for DMSO-d_6). Peak assignments are based on calculated chemical shifts, multiplicity and 2D experiments. IUPAC names of all compounds are provided and were determined using CS ChemBioDrawUltra 16. High-resolution mass spectra (HRMS) were recorded by staff at the Molecular and Bioanalytical (MoBiAS) center (ETH Zurich) employing a Bruker maXis-ESI-Qq-TOF-MS (ESI). Description of syntheses, spectroscopic characterization, and NMR spectra are reported in the Supporting information.

Optical spectroscopy

Stock solutions in DMSO were prepared at concentrations of 1–15 mM, stored at –20 °C and thawed immediately before each experiment. Spectroscopic measurements were conducted in phosphate-buffered saline (PBS) at pH = 7.4. UV-Visible spectra were obtained employing a Cary 500 Scan spectrometer using quartz cuvettes from Thorlabs (10 mm path length). Fluorescence spectra were acquired using a Fluorolog 3 fluorimeter (Horiba Jobin-Yvon) at the indicated temperature. Extinction coefficients were determined by linear fit of 4 different concentrations of the compound in PBS. Absolute fluorescence quantum yields were determined in PBS by means of an integrating sphere (Horiba Jobin-Yvon). All spectroscopic experiments were carried out in triplicate.

Enzyme kinetics

Michaelis–Menten kinetics experiments were performed by monitoring the formation of **2** at different concentrations of substrate **1** or **3** (2–60 μM), constant NTR (NfsB, Sigma, 2 $\mu\text{g mL}^{-1}$) and NADH (500 μM) concentrations in PBS at 37 °C. The initial velocities of enzymatic cleavage were obtained by monitoring the absorbance of **2** in the first 10 min of the enzymatic activation. Because the absorbance of **2** is directly proportional to its concentration, the absorbance could be expressed in terms of concentration and the initial velocities (V_0) at different concentrations of probe **1** or **3** could be calculated. The velocities were plotted against the initial concentrations of **1** or **3**. The data were fit using the Michaelis–Menten equation in Prism 7 (GraphPad) to give the Michaelis–Menten constant (K_m) and turnover number (k_{cat}).

Cloning

All plasmids were cloned by Gibson assembly.^[1] DNA encoding for mTurquoise2 was amplified from plasmid pmTurquoise2-ER (Addgene #36204) to generate an insert. Plasmids containing the gene of interest fused to another fluorescent protein were used to generate the backbone. These plasmids were CFP-Parkin (Addgene #47560) and pEGFP-LC3 (Addgene #24920). Primers for amplification (minimum 15 overlapping base pairs) were generated using SnapGene® and modified manually to minimize hairpins, homodimers, and repeating motifs. The designed primers (Table

S2) were supplied by Mycosynth AG (Switzerland). The amplified DNA fragments were generated by PCR using Phusion High-Fidelity PCR Master Mix with HF from New England Biolabs (NEB). The fragments were analyzed by gel electrophoresis and purified using QIAquick PCR purification kit (Qiagen) according to the manufacturer's instructions. The Gibson assembly reaction was performed using Gibson Assembly Master Mix (NEB). NEB DH5 α competent *E. coli* cells were transformed with the assembly product according to the manufacturer's protocol and streaked onto lysogeny broth (LB) agar plates containing kanamycin (50 $\mu\text{g mL}^{-1}$). After incubation at 37 °C for 24 h, single colonies were selected and grown in LB liquid medium containing 50 $\mu\text{g mL}^{-1}$ kanamycin at 37 °C for 16 h. Plasmid DNA was extracted and purified using QIAprep spin miniprep kit (Qiagen) according to the manufacturer's instructions and sequenced by Mycosynth AG (Switzerland). Plasmids are available from Addgene as pmTurquoise2-LAMP1^[2] (pmT-Lyso, #110948), pmTurquoise2-Parkin (pmT-Parkin, #110945) and pmTurquoise2-LC3 (pmT-LC3, #110947).

Cell culture

HEK293 cells were grown in Dulbecco's Modified Eagle Medium (DMEM) supplemented with fetal bovine serum (FBS, 10%) and penicillin-streptomycin (1%) at 37 °C in 5% CO₂ environment. The cells were split after 90% confluence was reached. For microscopy experiments, 20'000 cells per well were seeded onto 8-well plates (0.5 mL, Nunc Lab-Tek II or 0.3 mL, Ibidi chambered cover glass) 2–4 days prior to imaging. The probes were incubated in growth medium for the indicated time. Before imaging, the growth medium was removed and the cells were washed with PBS and imaged in imaging medium (FluoroBrite DMEM).

Cell viability assays

Cell viability assays. HEK293 cells were grown in DMEM supplemented with FBS (10%) and penicillin-streptomycin (1%) at 37 °C in 5% CO₂ environment. The cytotoxicity of the probes was determined by methylthiazolyldiphenyl-tetrazolium bromide (MTT) colorimetric assays. MTT is reduced to the purple tetrazolium salt formazan in living cells. 9'000 cells were seeded onto each well of a 96-well plate and grown for 24 h at 37 °C, 5% CO₂. The compounds were incubated for 48 h at different

concentrations ranging from 100 nM to 100 μ M. Stock solutions of the compounds were prepared in DMSO and cells were incubated in growth medium with a final DMSO concentration of 0.5%. Positive control with 0.5% DMSO in growth medium was taken as the reference for 100% cell viability. After 48 h of incubation, the cells were treated with 10% MTT solution (5 mg mL⁻¹ in FluoroBrite DMEM) and incubated for 3 h. The medium was then removed carefully and 2-propanol (100 μ L per well) was added to dissolve the formazan. The plates were shaken at 450 rpm for 30 min and the absorbance was measured at 550 nm, using a plate reader (SPARK 10M, TECAN Group AG). Biological triplicates, each measured three times ($N = 9$), for each compound were recorded for each concentration and IC₅₀ values were determined using Prism 7 (Graph Pad) fit with a four parameters logistic regression.

Confocal fluorescence microscopy

Imaging was performed with a spinning disk confocal (Nikon) or confocal (Olympus and Leica) microscopes.

The Nikon Eclipse T1 spinning disk light microscope is equipped with a Yokogawa confocal scanner unit CSU-W1-T2 and two sCMOS (Orca Flash 4.0 V2) or EMCCD (iXon 888) cameras. Light sources: Diode-pumped solid-state (DPSS) 405 nm (120 mW, 20-40% laser power, 1-2 s exposure time), DPSS 445 nm (100 mW, 20-40%, 1-2 s), diode 561 nm (200 mW, 20-40%, 1-2 s) and 640 nm (150 mW, 40%, 2 s). All images were collected using an oil-immersion 100 \times CFI Apo TIRF (NA = 1.49) objective. The following emission filters were used: ET450/50, ET470/24, ET 630/75, and ET700/75. The microscope was operated using VisiVIEW (Metamorph) software.

The Olympus FluoView 3000 IX83 laser scanning confocal microscope is a fully-motorized and automated inverted setup. It is equipped with 4 GaAsP photomultiplier tubes (PMT, spectral detection option) and 1 transmission PMT. Light sources: LED based (CoolLED pE300white) unit for conventional epi-illumination for visual observation. All images were collected using a silicon-immersion 60 \times Silicon UPlanSApo (NA = 1.3) objective. The microscope was operated using FV3000 system (FV31S-SW, CellSens) software.

The Leica SP8 system is a fully-motorized and automated inverted microscope equipped with 2 photomultiplier tubes (PMT) detectors, 2 hybrid detectors (HyD) and

1 HyD single-molecule detection (HyD SMD) for fluorescence and a PMT transmission light detector. Spectral detector ranges from 380 nm to 800 nm. Light sources: 405 nm fixed wavelength (diode laser) and variable white light laser: tunable from 470 nm to 670 nm in 1 nm increments. All images were collected using an HC PL Apo, oil-immersion, 63 \times magnification, NA = 1.40 objective. Image size: 1024 \times 1024 pixels (pixel size = 12.75 μm^{-1}). The microscope was operated using LAS X software. Image analysis was carried out using Fiji (ImageJ 1.5d, NIH). To determine intracellular fluorescence intensity, the cell body was selected as the region of interest (ROI) and the integrated intensity within the ROI was measured. An additional ROI of the same size and shape was used to obtain the integrated intensity of the background (region with no cell). The background intensity was subtracted from that of the cell-containing ROI. The analyses were plotted using Prism 7 (GraphPad).

Co-localization experiments

HEK293 cells were transfected 24–48 h before imaging using plasmids obtained from Addgene (abbreviation, #plasmid): pmTurquoise2-ER (pmT-ER, #36204), pmTurquoise2-Mito (pmT-Mito, #36208), pmTurquoise2-Golgi (pmT-Golgi, #36205)^[3] or employing our own assembled plasmids (available from Addgene): pmTurquoise2-LAMP1 (pmT-Lyso, #110948), pmTurquoise2-Parkin (pmT-Parkin, #110945) and pmTurquoise2-LC3 (pmT-LC3, #110947). Cells were transfected employing the jetPRIME kit according to the instructions from the manufacturer (Polyplus) and the medium was replaced with fresh growth medium after 4–5 h. For nucleus co-localization, cells were stained with Hoechst 33342 (5 μM) for at least 30 min prior to imaging. For small-molecule mitochondria co-localization, cells were incubated with MitoTracker™ Deep Red FM (MDR, Thermo Fisher, 20 nM) for 1 h prior to incubation with the probes. Compound **1** or **5** were added 1–3 h prior to imaging. Fluorescent emission of the activated probes (561 nm, 2 s exposure time, 40% laser power), of the mTurquoise2-tagged protein (445 nm, 2 s, 40%), Hoechst (405 nm, 1 s, 40%) and MDR (640 nm, 2 s, 40%) were recorded. Pearson's coefficients were calculated by selecting a transfected cell as ROI and running the co-localization studio plugin contained in the image analysis program ICY (GPLv3, Institute Pasteur).

LC-MS analysis

The procedure for the determination of intracellular concentrations of dye **2** by LC-MS analysis of cell lysates was adapted from a published method.^[4] HEK293 cells were grown in DMEM supplemented with FBS (10%) and penicillin-streptomycin (1%) at 37 °C in 5% CO₂ environment. Cells were seeded in T75 flasks (75 cm²), grown to 90% confluency, and incubated with the compounds for the indicated times and concentrations. Cells were trypsinized, counted and pelleted and the medium was removed gently without disturbing the cell pellet. The cells were washed once with 1 mL of growth medium to avoid reducing the estimated concentration due to rapid diffusion of small molecules. The medium was removed and 200 µL of water/methanol (40:60) were added to the cell pellet, which was re-suspended by dragging the tube on a rough surface (no mixing with pipet). The cells were lysed by freeze-thaw cycles alternating 3 min in liquid nitrogen with thawing in water bath (room temperature) for 10 cycles. The lysate was vortexed and centrifuged for 30 min at 4 °C. The supernatant was transferred to a new tube and centrifuged for 30 min at 4 °C. The supernatant was transferred to a 3K MWCO Amicon tube and centrifuged for 30 min at 4 °C to remove molecules with a molecular weight over 3 kDa. The flow-through was stored at -20 °C or used directly and pipetted into an LC-MS insert. Control lysates (no compound incubation) were combined and aliquoted (5 × 20 µL). The samples were analyzed by LC-MS using the selected ion monitoring (SIM) mode for the molecular weight of reporter **2** ($m/z = 277.5$) and monitoring at 501 nm, near the absorption maximum. A calibration curve was built by addition of known amounts of probe **2** to control cell lysate to generate solutions of known concentrations of **2**. The intracellular concentration of dye **2** resulting from activation of probe **1** or **3** was calculated based on the calibration curve, using the absorbance peak area, total volume of lysate and total number of cells. From each sample, 2 µL were injected into a Waters Acquity H-class UPLC connected to a Water SQ Detector 2. The prepared sample was separated on a Waters BEH C18 1.7 µm column with an acetonitrile (ACN)/water/0.1% formic acid (FA) solvent system. Starting conditions were kept for 2 minutes at 99.9% water in 0.1% FA. In 2 minutes, the gradient was linearly ramped to 98% ACN in 0.1% FA. This condition was kept for 5 min before returning to starting conditions. The single quadrupole detector scanned alternatively between full scan (120-650 m/z) and SIM

mode, monitoring 277.5 m/z with a dwell time of 0.125 s. Cone voltage was kept constant at 35 V.

Mitochondrial glutathione redox states in live cells

Live HEK293 cells were seeded on Ibidi plates 3 days prior imaging. The cells were transfected with pLPCX mito Grx1-roGFP2 (Addgene #64977) 2 days prior imaging. The medium was removed, the cells were washed with PBS and incubated with the corresponding compounds at the indicated concentrations in FluoroBrite DMEM (probe **1**: 15 μ M, probe **3**: 5 μ M). Image analysis was carried out using Fiji (ImageJ 1.5d, NIH). To determine fluorescence intensity, the cell body was selected as ROI and the integrated intensity (500-530 nm) upon excitation at 405 nm within the ROI was measured. An additional ROI of the same size and shape was used to obtain the integrated intensity of the background (region with no cell). The background intensity was subtracted from that of the cell-containing ROI. The same ROI and background were selected in the imaged obtained upon excitation at 488 nm. The ratio of the background corrected 405/488 nm image was then calculated. The analyses were plotted using Prism 8 (GraphPad).

Labeling of free nucleophilic thiols in proteomes of treated cells

Cell lysates: HEK293 cells were grown in DMEM supplemented with FBS (10%) and penicillin-streptomycin (1%) at 37 °C in 5% CO₂ environment. The cells were seeded in a T25 flask and after 90% confluence was reached, they were treated with the indicated compounds in growth medium: probe **1** (15 μ M, 3 h), probe **3** (5 μ M, 3 h), DMSO (0.5% v/v, 3 h), then washed with PBS. The cells were trypsinized and centrifuged, and the medium was removed. The cells were re-suspended in cold PBS, centrifuged and PBS was removed carefully without disturbing the cell pellet. The cells were re-suspended in 200 μ L of water/methanol (40:60) containing Protease Inhibitor Cocktail (Sigma-Aldrich, P8340) and iodoacetamide alkyne (IAA) (100 μ M) except for the alkyne-free sample. The cells were lysed by freeze-thaw cycles alternating 3 min in liquid nitrogen with thawing in water bath (room temperature) for 10 cycles. The lysate was vortexed and centrifuged for 30 min at 4 °C (21'000 \times g). The supernatant was transferred to a new tube and centrifuged for 30 min at 4 °C (21'000 \times g). The

supernatant was transferred to a 3K MWCO Amicon tube and centrifuged for 30 min at 4 °C ($14'000 \times g$) to separate the proteins from molecules with a molecular weight under 3 kDa. The flow-through was discarded and the protein concentration was determined by BCA assay, the samples were stored at -20 °C for later use.

Click-reaction: The protein concentrates were thawed on ice. The click-mix solution containing 1.25 mM CuSO₄, 2.5 mM bathophenanthroline disulfonic acid (BPSA) and 20 mM sodium ascorbate was prepared. For each reaction, the following was added to an Eppendorf tube: 45 μ L of protein concentrate (1–5 mg/mL), 1 μ L of 1 mM azide-functionalized carboxy-X-rhodamine, 4 μ L of the click-mix and the tube was gently flicked to avoid air bubbles. The reaction was incubated for 1 h, at 4 °C and allowed to proceed protected from light.

Sample preparation for gel analysis: 150 μ L of methanol were added to 50 μ L of reaction mixture, vortexed briefly. 40 μ L of chloroform were added, vortexed briefly. The Eppendorf tube was centrifuged for 5 min at $13'000 \times g$ and the upper aqueous layer was removed. 120 μ L of methanol were added and vortexed briefly. The solution was centrifuged for 5 min at $13'000 \times g$ to pellet proteins and the supernatant was removed. 120 μ L of methanol were added, vortexed briefly, centrifuged for 5 min at $13'000 \times g$ to pellet proteins, and the supernatant was removed. The protein pellet was allowed to air-dry for at least 15 min. The samples were capped and stored at -20 °C until ready for use.

Gel analysis: The proteins were loaded on 10-well gels from BioRad (4–20% Mini-PROTEAN® TGX™ Precast Protein Gels, 10-well, 30 μ L) and ran at 200 V for 40 min in TGS running buffer. The fluorescence was read at 560 nm with a ChemiDoc™ MP Imaging Systems (BioRad) and the band intensities were measured using Fiji software.

Superoxide production and BSO experiment

Live HEK293 cells were seeded on Ibidi plates 2 days prior to imaging. The cells were incubated with BSO for 3 h, washed with PBS and co-incubated with BSO (250 μ M) and the corresponding compounds at the indicated concentrations for another 3 h. The medium was removed, the cells were washed with PBS, incubated with superoxide sensor (10 μ M) for 30 min in FluoroBrite DMEM and imaged. Image analysis was carried out using Fiji (ImageJ 1.5d, NIH). To determine intracellular

fluorescence intensity, the cell body was selected as ROI and the integrated intensity within the ROI was measured in the green channel. An additional ROI of the same size and shape was used to obtain the integrated intensity of the background (region with no cell). The background intensity was subtracted from that of the cell-containing ROI. The analyses were plotted using Prism 7 (GraphPad).

Quantitative image analysis of cell morphologies and mitochondrial/cytosolic ratios

Automatic identification of mitochondria, vesicles and cytosolic space from micrographs was carried out employing homemade macros running on the Fiji platform. The code and a tutorial-like description of how they were used are provided in the SI.

Total RNA isolation

HEK293 cells were grown in DMEM supplemented with FBS (10%) and penicillin-streptomycin (1%) at 37 °C in 5% CO₂ environment. The cells were seeded in a T75 flask and after 90% confluence was reached, the cells were treated with the indicated compounds for 3 h: DMSO (1% v/v), probe **1** (15 μM), or probe **3** (5 μM). The cells were trypsinized and centrifuged, and the medium was removed. The cells were re-suspended in PBS, centrifuged and PBS was removed carefully without disturbing the cell pellet. RNA was extracted from the treated cells using RNeasy® Plus Mini Kit (Qiagen) following the manufacturer's instructions. In brief, buffer RLT Plus (lysis buffer) was added to the cell pellet and homogenized. The homogenized lysate was transferred to a gDNA Eliminator spin column, centrifuged and the flow-through was saved. One volume of 70% ethanol was added to the flow-through, mixed and transferred to an RNeasy Mini spin column, centrifuged and the flow-through was discarded. Buffer RW1 (wash buffer containing guanidine salt, removing carbohydrates, proteins and fatty acids) was added to the column, centrifuged and the flow-through was discarded. Buffer RPE (wash buffer, removing traces of salts) was added to the column, centrifuged and the flow-through was discarded. This last step was repeated and the column was centrifuged again to further dry the membrane. RNase-free water was added to the column and centrifuged to elute the RNA. The quantity and purity of each RNA sample was assessed by measuring the absorbance at 260 nm using a Nanodrop spectrophotometer as well as using an Agilent® 2100

Bioanalyzer®. The samples were stored at $-80\text{ }^{\circ}\text{C}$ and handed to the Functional Genomics Center Zurich (FGCZ), where library generation, sequencing and preliminary bioinformatic analyses were carried out.

mRNA library preparation for sequencing

The quality of the isolated RNA was determined with a Qubit® (1.0) Fluorometer (Life Technologies, California, USA) and a Bioanalyzer 2100 (Agilent, Waldbronn, Germany). Only those samples with a 260/280 nm ratio between 1.8–2.1 and a 28S/18S ratio within 1.5–2 were further processed. The TruSeq RNA Sample Prep Kit v2 (Illumina, Inc, California, USA) was used in the succeeding steps. Briefly, total RNA samples (100–1000 ng) were poly A-enriched and then reverse-transcribed into double-stranded cDNA. The cDNA samples were fragmented, end-repaired and polyadenylated before ligation of TruSeq adapters containing the index for multiplexing. Fragments containing TruSeq adapters on both ends were selectively enriched by PCR. The quality and quantity of the enriched libraries were validated using Qubit® (1.0) Fluorometer and the Caliper GX LabChip® GX (Caliper Life Sciences, Inc., USA). The product was a smear with an average fragment size of approximately 260 bp. The libraries were normalized to 10 nM in Tris-Cl 10 mM, pH 8.5 with 0.1% Tween® 20.

Cluster generation and sequencing

The TruSeq PE Cluster Kit HS4000 or TruSeq SR Cluster Kit HS4000 (Illumina, Inc, California, USA) was used for cluster generation using 10 pM of pooled normalized libraries on the cBOT. Sequencing was performed on the Illumina HiSeq 2000 paired end at 2101 bp or single×101 bp or single end 100 bp using the TruSeq SBS Kit HS4000 (Illumina, Inc, California, USA).

Bioinformatic analysis

Reads were quality-checked with FastQC. Sequencing adapters were removed with Trimmomatic^[5] and reads were hard-trimmed by 5 bases at the 3'-end. Successively, reads at least 20 bases long, and with an overall average Phred quality score greater than 10 were aligned to the reference genome and transcriptome of Homo Sapiens

(FASTA and GTF files, respectively, downloaded from GRCh38) with STAR v2.5.1^[6] with default settings for single end reads. Distribution of the reads across genomic isoform expression was quantified using the R package GenomicRanges^[7] from Bioconductor Version 3.0. Differentially expressed genes were identified using the R package edgeR^[8] from Bioconductor Version 3.0. A gene is marked as differentially expressed (DE) if it possesses the following characteristics: at least 10 counts in at least half of the samples in one group, $P \leq 0.001$ and fold change ≥ 1.41 .

Probes Properties

Spectroscopic Properties

	ϵ ($M^{-1}cm^{-1}$)	$\lambda_{max,abs}$ (nm)	ϕ_{em} (%)	$\lambda_{max,em}$ (nm)	$\epsilon \times \phi_{em}$ ($M^{-1}cm^{-1}$)
probe 1	27840	285	0	-	-
probe 3	19627	378	0	-	-
probe 2	38416	481	0.18	555	6915

Table S1. Photophysical properties of probes measured in phosphate-buffered saline (PBS, 5 μ M).

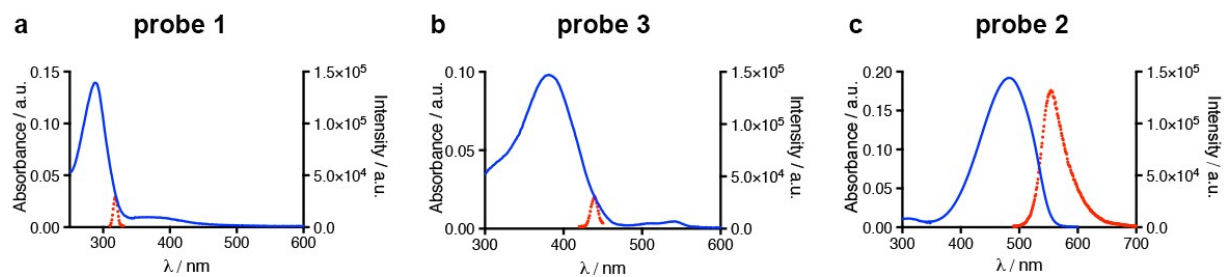


Figure S1. Absorption and fluorescence spectra of the probes **1**, **2** and **3**. Absorption (blue) and fluorescence (red) spectra of the probes (5 μ M) in PBS. **a**, Spectra of probe **1**. **b**, Spectra of probe **3**. **c**, Spectra of probe **2**.

Kinetic Properties

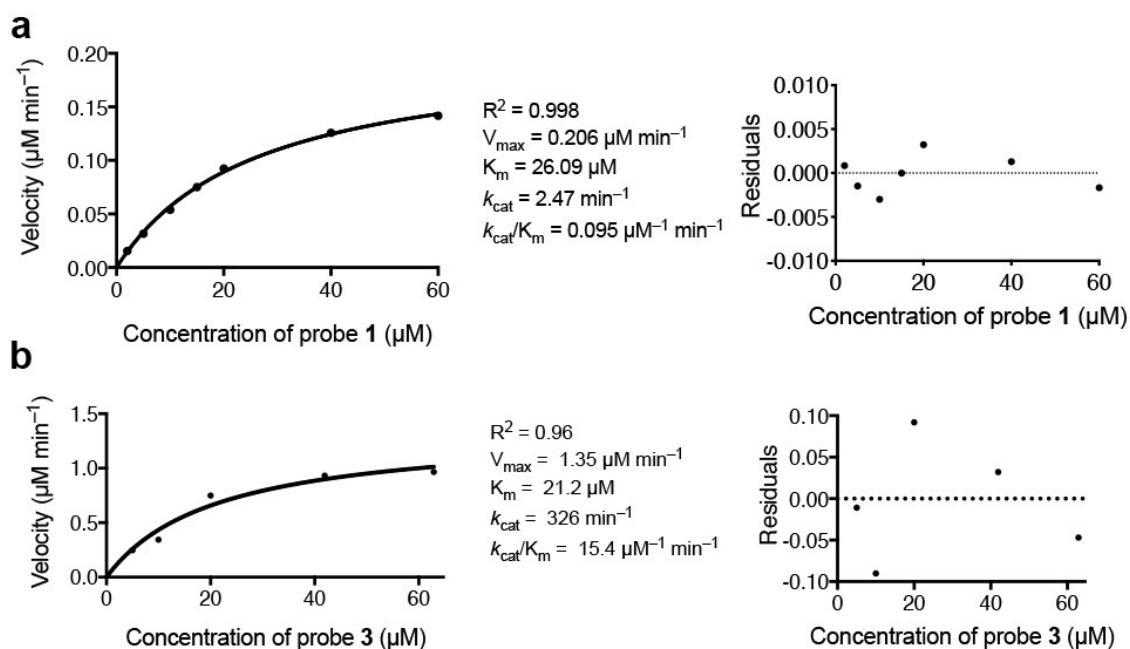


Figure S2. Michaelis-Menten kinetics of activation of probes **1** and **3** by bacterial nitroreductase (NfsB from *E. coli*). **a**, Activation of probe **1**. **b**, Activation of probe **3**. In both cases, the absorbance of reported dye **2** was followed, giving the overall kinetics of reduction of the nitro group to amine, and release of phosphine (extremely fast step for compound **1**). The residual plots of both **a** and **b** are shown on the right side of each activation plots to show how well the data follows the Michaelis-Menten model, with small positive and negative values.

Live Cells and Lysates

Co-localization analysis

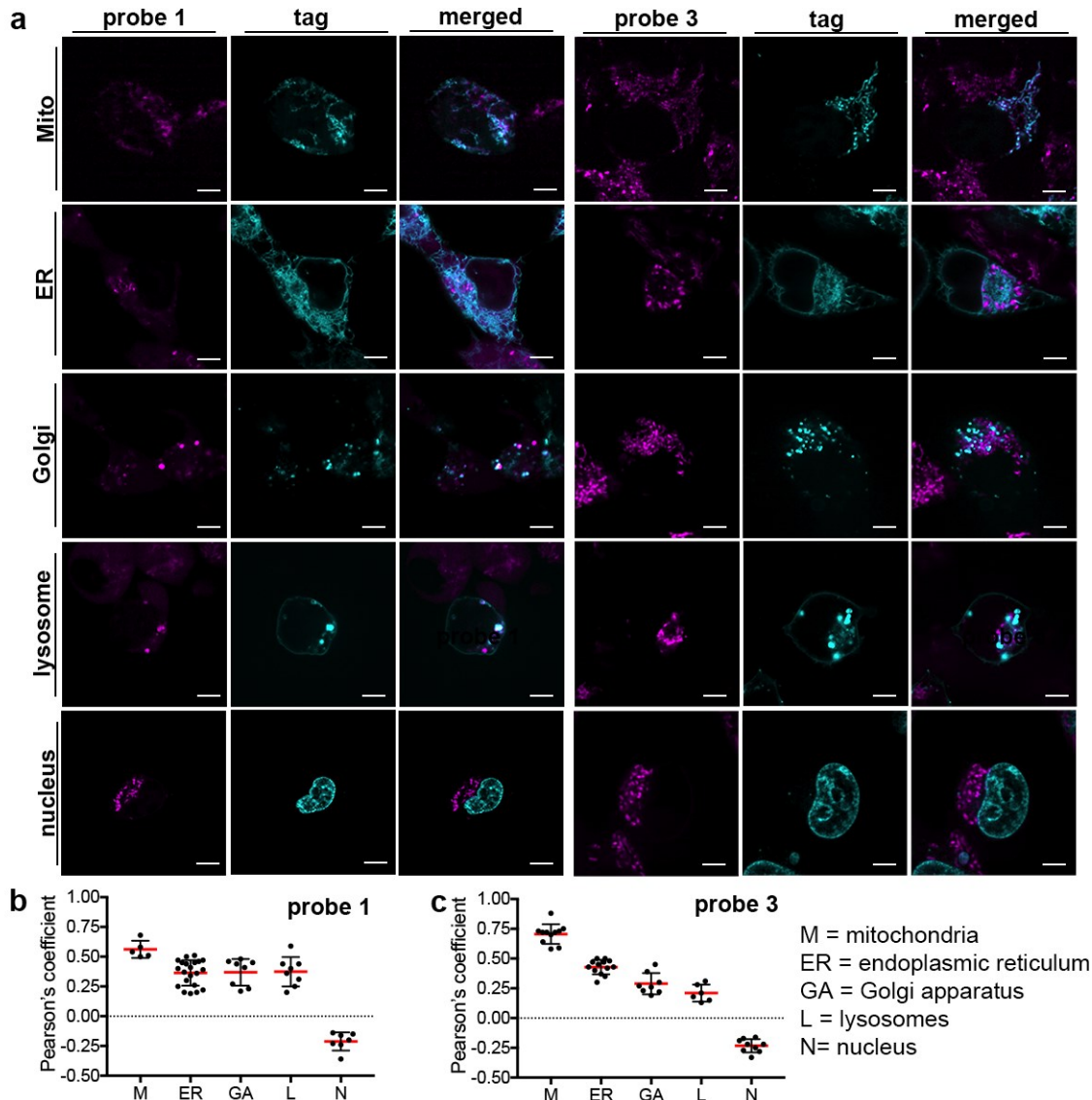


Figure S3. Co-localization of reporter dye **2** and organelle-targeted mTurquoise2. **a**, HEK293 cells were incubated with Hoechst dye (5 μ M), transfected with plasmids pmT-Mito, pmT-ER, pmT-Golgi or pmT-Lyso. The cells were incubated with probe **1** (left) and **3** (right). Scale bar = 10 μ m. **b**, Pearson's correlation coefficients of probe **1**, $N > 5$ cells from three biological replicates. **c**, Pearson's correlation coefficients of probe **3**, $N > 6$ cells from three biological replicates. For both probes, reporter dye **2** is generated in mitochondria. The nucleus tag is Hoechst 33342 and mTurquoise2 for the other organelles.

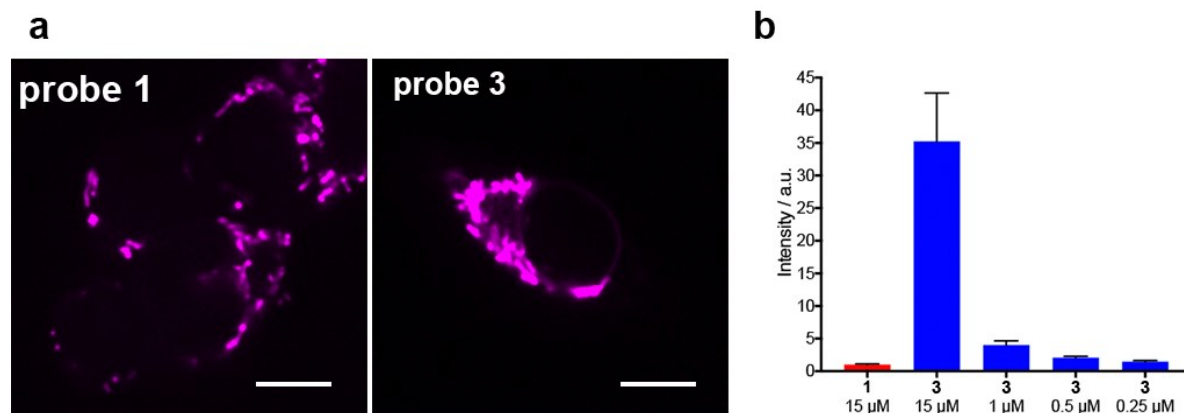
Fluorescence Intensities

Figure S4. Relative fluorescent intensities of intracellular activation of probes **1** and **3**. **a**, Intracellular fluorescence upon enzymatic activation of compounds **1** (15 μ M) or **3** (0.5 μ M) in live HEK293 cells. Fluorescence intensity was measured in the red channel (excitation: 561 nm, identical settings for both compounds). Scale bar = 10 μ m. **b**, Relative fluorescence intensities of probe **3** at concentrations ranging from 15 μ M to 0.25 μ M (blue) compared to probe **1** at 15 μ M (red) after 1 h incubation. Bars indicate average of relative intensity of cells when treated with **3**, relative to **1** at 15 μ M (intensity = 1). Measurements of $N > 10$ cells from biological replicates. Error bars represent 95% confidence ranges.

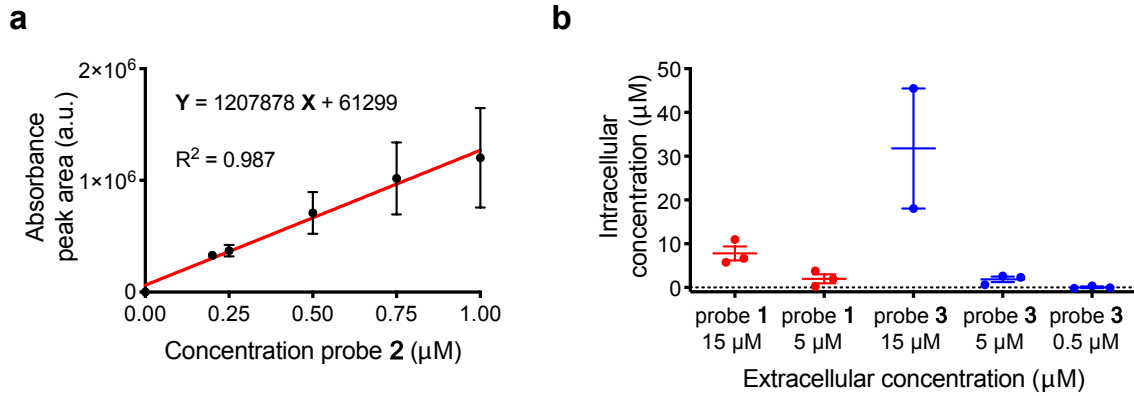
Intracellular Concentration

Figure S5. Intracellular concentrations of reporter dye **2** upon treatment of cells with probes **1** or **3**, measured by LC-MS SIM. **a**, Calibration curve. Control lysates spiked with probe **2** at the indicated concentrations. Absorbance peak areas were used to determine concentrations. **b**, Intracellular concentrations of probes **1** and **3** after incubation at the indicated extracellular concentrations for 3 h. Lysates and calibration curves are from three biological replicates ($N = 3$), error bars are standard deviation of the mean. This experiment reveals that at extracellular concentrations of 15 μM, the intracellular production of **2** from **3** is much greater than from probe **1**, in agreement with the more intense fluorescence observed in the microscopy experiment (Figure S4). Aiming at finding a compromise between the fluorescence and LC-MS experiments, we decided that an extracellular concentration of 15 μM of **1** and 5 μM of **3** gives roughly equivalent intracellular concentrations of **2**.

Cell Viability Assays

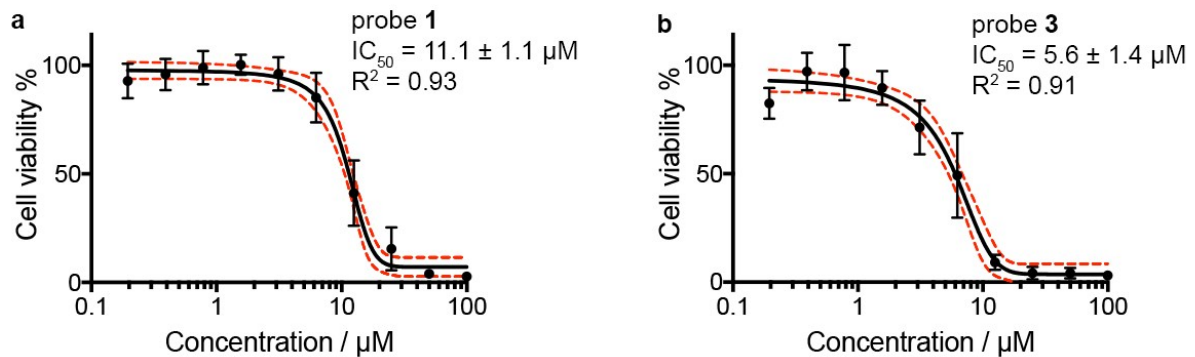


Figure S6. Cell viability assays. HEK293 cells were incubated with **a**, probe 1 or **b**, probe 3 at concentrations ranging from 100 nM to 100 μM for 48 h. The cells were then incubated with MTT solution and the absorbance of formazan was measured at 550 nm. DMSO control (0.5%) sets the 100% viability. Black points are averages of nine measurements (triplicates of triplicates). Black lines are four parameters logistic regression (4PL) fit. Error bars represent 95% confidence ranges. Red dashed lines are 95% confidence interval bands.

Mitochondrial redox state: roGFP2 sensor

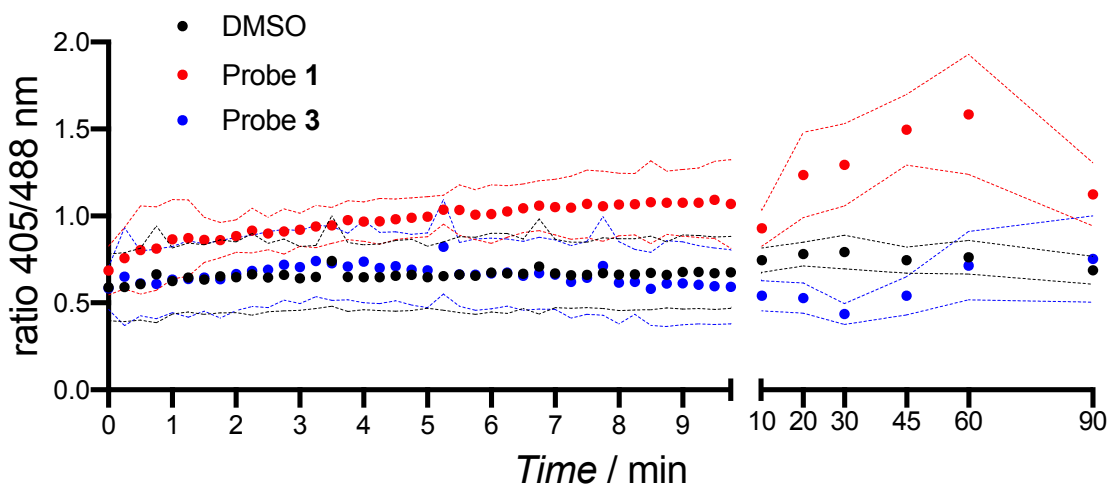


Figure S7. Mitochondrial glutathione redox states determined using Grx1-roGFP2 ratiometric sensor. Ratio of integrated fluorescence intensities (500–530 nm) measured upon excitation at 405 or 488 nm. Means are plotted and lines represent 95% confidence intervals. Measurements were carried out in biological duplicates and data from $N > 5$ cells were employed.

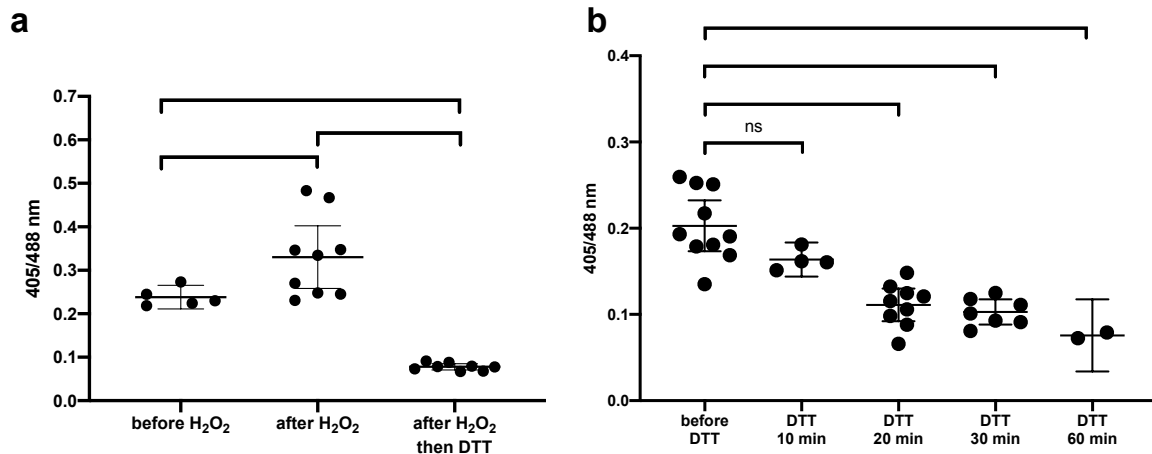


Figure S8. Mitochondrial glutathione redox states determined using Grx1-roGFP2 ratiometric sensor. **a**, before any treatment, after treatment with 0.5 mM H₂O₂ for 5 min, followed by treatment with 5 mM DTT for 5 min. **b**, before and after treatment with 5 mM dithioreithol (DTT) at the indicated incubation times. Ratio of integrated fluorescence intensities (500–530 nm) measured upon excitation at 405 or 488 nm. Means are plotted and lines represent 95% confidence intervals. Measurements were carried out in a single biological experiment and each dot represents one cell. Statistical significance was assessed by unpaired, two-tailed, Mann–Whitney test. P values: **** < 0.0001, ** < 0.001, * < 0.05 and ns = not significant.

Mitochondrial redox state: small molecule sensor

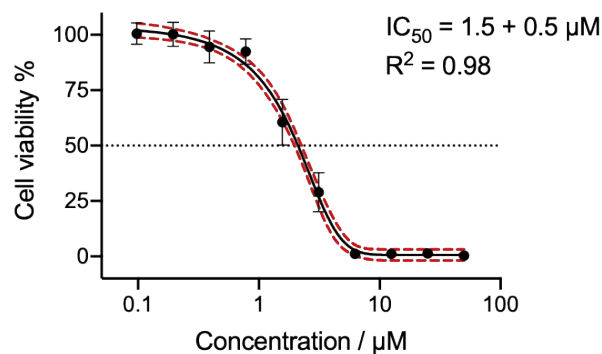


Figure S9. Cell viability assays. HEK293 cells were incubated with the mitochondrial GSH/GSSG ratiometric sensor at concentrations ranging from 100 nM to 50 μM for 48 h. The cells were then incubated with MTT solution and the absorbance of formazan was measured at 550 nm. DMSO control (0.5%) sets the 100% viability. Black points are averages of 3 measurements (triplicates). Black lines are four parameters logistic regression (4PL) fit. Error bars represent 95% confidence ranges. Red dashed lines are 95% confidence interval bands.

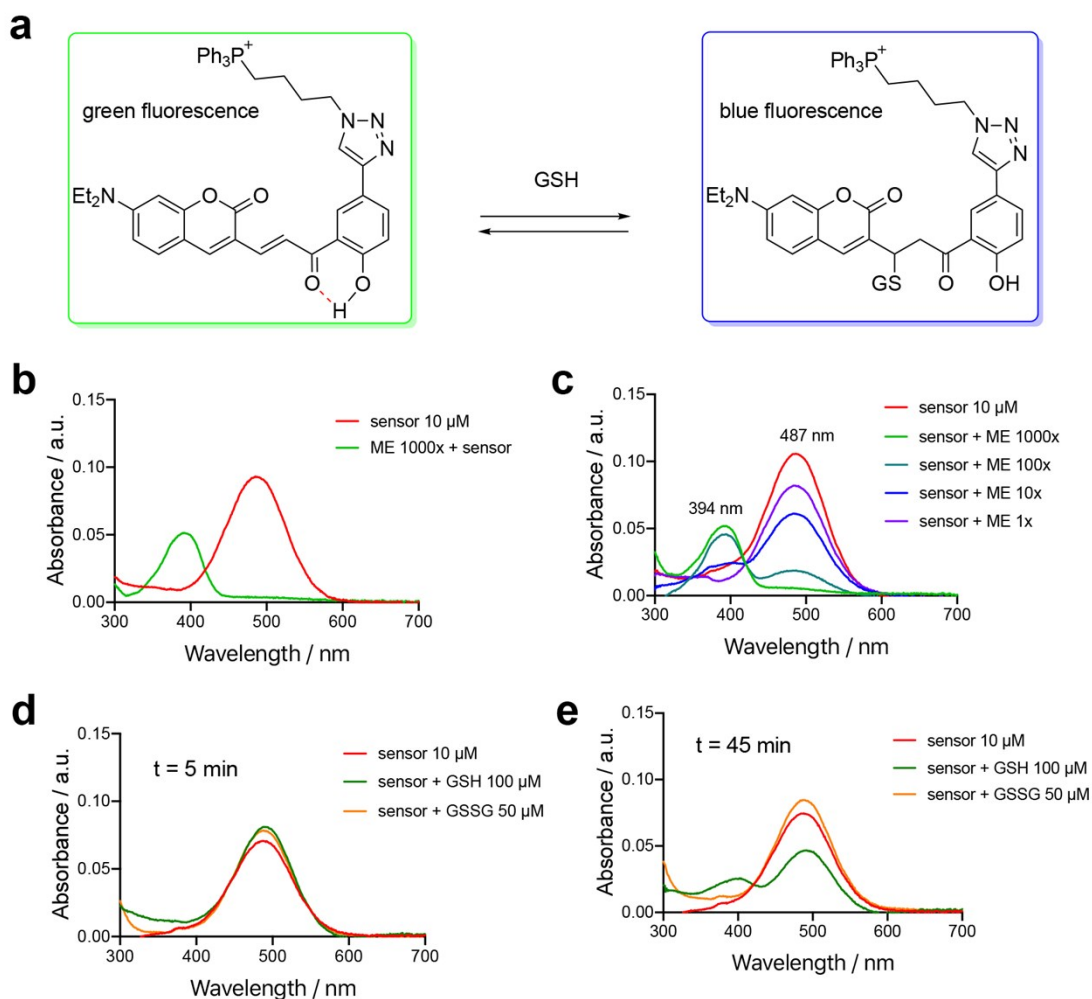


Figure S10. Structure and response of a mitochondria-targeted fluorescent sensor for GSH/GSSG ratio. **a**, Structure of the probe and mechanism of GSH sensing. **b**, Absorption spectra of mitochondria GSH/GSSG ratiometric sensor upon addition with 2-mercaptoethanol (ME). The absorbance is blue-shifted upon addition of ME. **c**, Ratiometric response upon addition of ME (1 to 1000 equivalents). **d** and **e**, Time-dependent response upon addition of GSH (100 μM) or GSSG (50 μM). Spectra were recorded in DMSO/PBS (4:1, v/v) at 25 $^{\circ}\text{C}$.

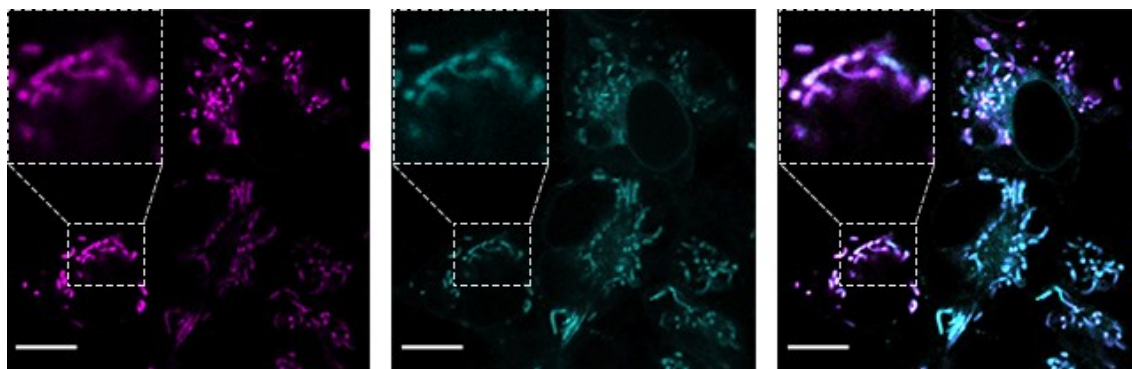


Figure S11. Co-localization of GSH/GSSG ratiometric sensor (cyan) with mitochondria using Mitotracker Deep Red (MDR, magenta) in live HEK293 cells. Scale bar = 10 μm .

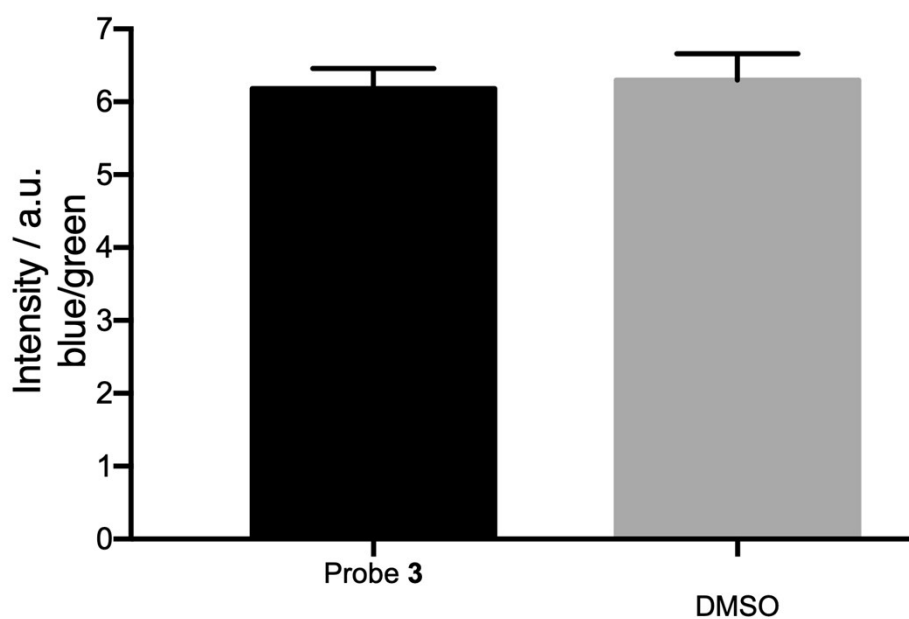


Figure S12. Ratio of blue to green fluorescence in cells treated with a GSH/GSSG sensor (see Figure S10) and either probe **3** (15 μM) or an equivalent amount of DMSO. Means are plotted and errors bars represent 95% confidence ranges.

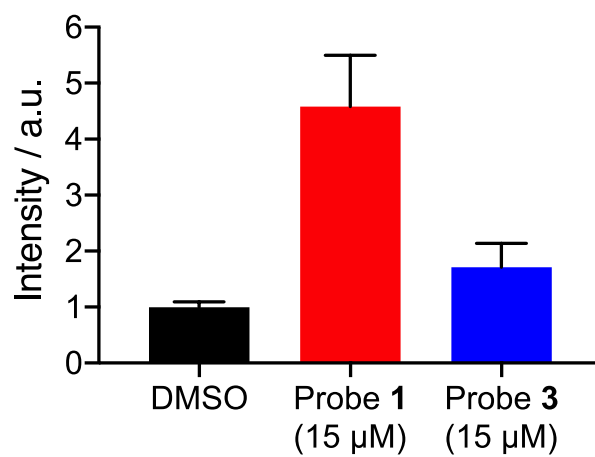
Superoxide Production

Figure S13. Production of superoxide, measured by the fluorescent sensor HK-SOX-1, induced by probe 1 and probe 3, both at an incubation concentration of 15 μM.

Labeling of Free Thiols in the Proteome

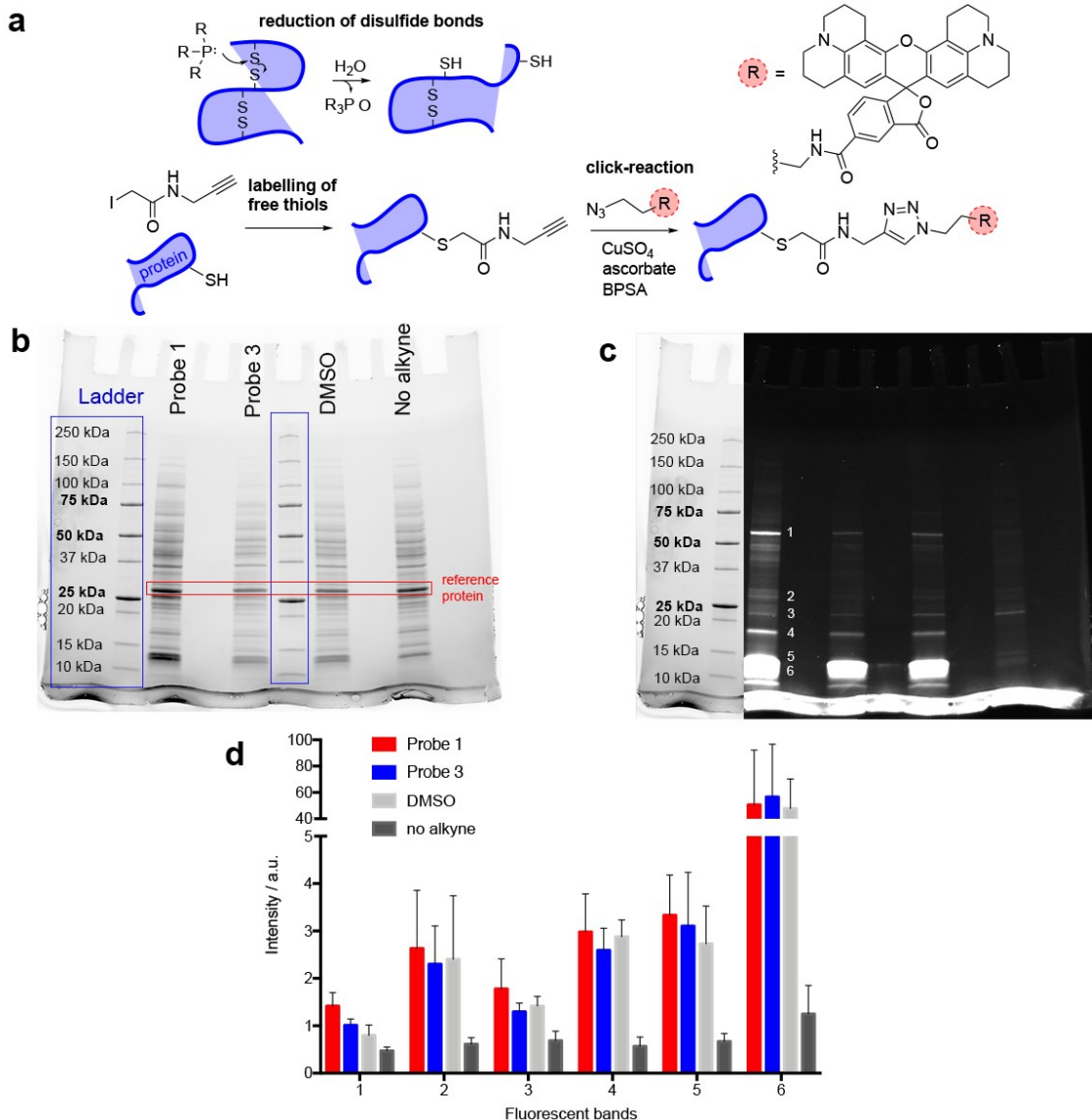


Figure S14. Tributylphosphine does not reduce disulfide bonds in proteins. **a**, Mechanism of action of proteins disulfide bonds reduction by trialkylphosphines and experimental procedure of labeling of free thiols by iodoacetamide alkyne (IAA) in cell lysates followed by click-reaction with a fluorescent reporter. **b**, image of stain-free gel and **c**, fluorescent image (same gel), of HEK293 whole cell lysates treated with probe **1** (15 μ M), probe **3** (5 μ M) and DMSO (0.5%) for 3 h, lysed and immediately labeled with IAA, followed by click-reaction with fluorescent reporter. The protein ladder (**b**, blue rectangle) is reported on the fluorescent image (**c**) for ease of observation. The reference protein (**b**, red rectangle) is used to normalize the band intensities in each sample based on the stain-free gel image. The bands quantified are numbered (**c**, white numbers). **d**, quantification of fluorescence intensity. Measurements were

carried out in biological triplicates. Bars represent means and error bars represent 95% confidence intervals. Statistical significance was assessed by unpaired, two-tailed, Mann-Whitney test. None of the comparisons displayed statistical significance, P values > 0.05 .

Mitochondrial Morphology

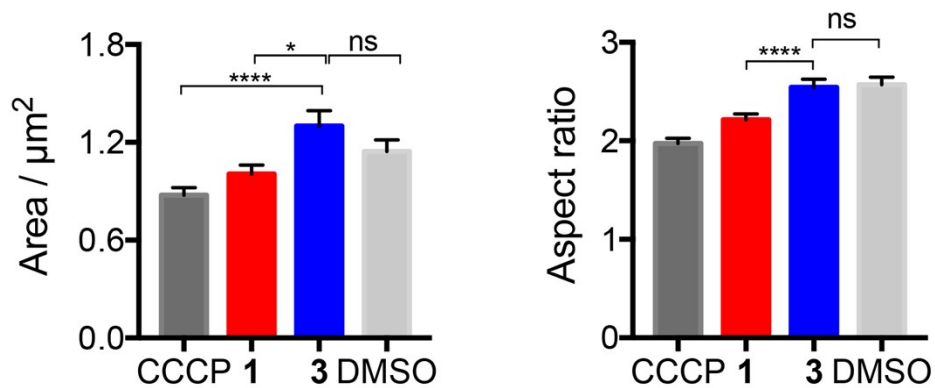


Figure S15. Analysis of mitochondrial shapes after treatment with CCCP (20 μM , 2 h), probe **1** (15 μM , 3-4 h), probe **3** (5 μM , 3-4 h), or DMSO (1%, 3-4 h). Measurements were carried out in biological triplicates and morphological data from $N = 1000$ mitochondria were employed for each condition. Means are plotted and error bars represent 95% confidence intervals. Statistical significance was assessed by unpaired, two-tailed, Mann-Whitney test. P values: **** < 0.0001 , * < 0.05 , ns = not significant > 0.05 .

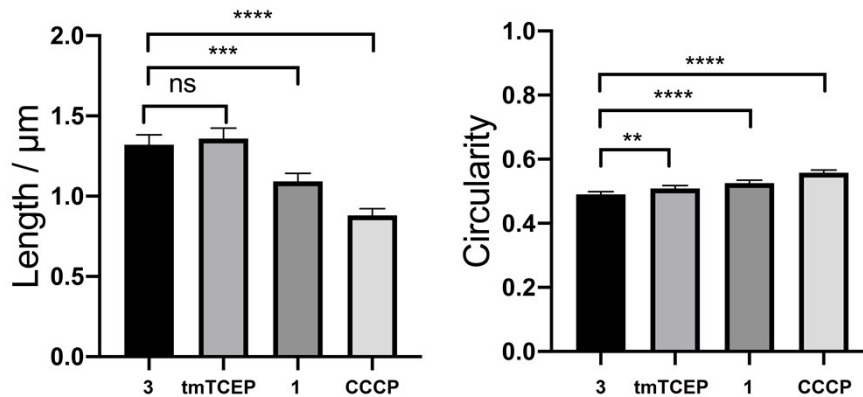
Mitochondrial Morphology tmTCEP

Figure S16. Analysis of mitochondrial shapes after treatment with CCCP (20 μ M, 2 h), probe **1** (15 μ M, 3 h), probe **3** (5 μ M, 3 h), or tmTCEP (15 μ M, 3 h). Measurements were carried out in biological triplicates and morphological data from $N > 1000$ mitochondria were employed for each condition. Means are plotted and errors bars represent 95% confidence intervals. Statistical significance was assessed by unpaired, two-tailed, Mann-Whitney test. P values: **** < 0.0001, *** < 0.001, ** < 0.01, ns = not significant > 0.05.

Plasmid Maps

Plasmid maps of assembled mTurquoise2-Parkin and mTurquoise2-LC3 are shown in Figure S11 and primers used in Table S2.

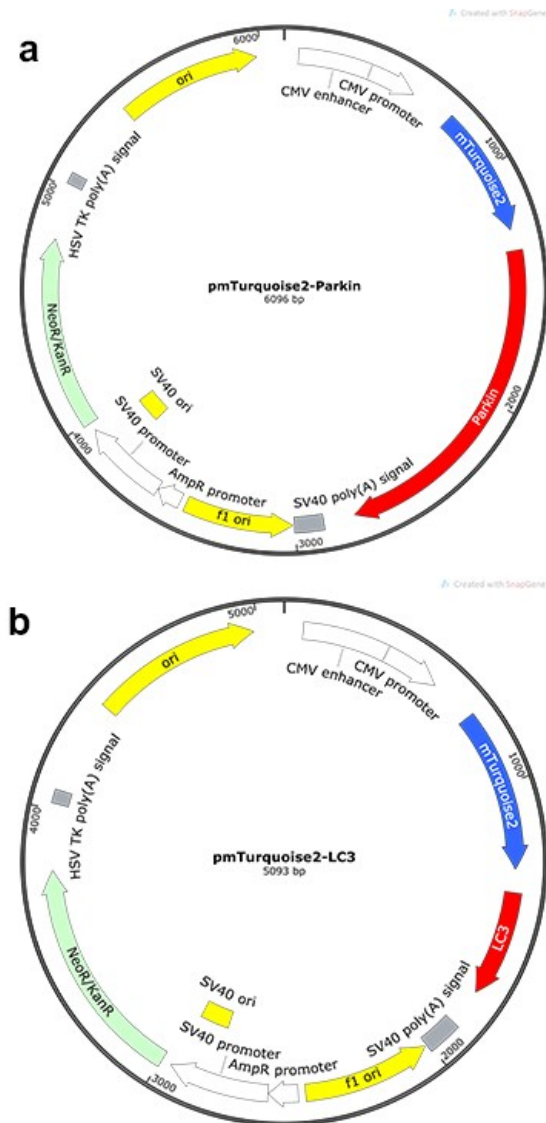


Figure S17. Plasmid maps of Gibson assembly constructs. mTurquoise2 fluorescent tags are depicted in blue and the proteins of interest in red. General features, selective markers and promoters are also depicted on the maps. **a**, pmTurquoise2-Parkin: mammalian expression of Parkin fused to mTurquoise2. **b**, pmTurquoise2-LC3: mammalian expression of LC3 fused to mTurquoise2. Maps were generated using SnapGene® 4.1.9.

Table S2. PCR primers used for the Gibson assemblies of pmTurquoise2-LC3 and pmTurquoise2-Parkin.

	primer name	direction	primer sequence: 5'- to -3'
pmTurquoise2-Parkin	pmt-PARK-BB.for	forward	GCG CGA TCA CAT GGT CCT G
	pmt-PARK-BB.rev	reverse	GCA GAT GAA CTT CAG GGT CA
	PMT-park-INS.for	forward	CCC TGA AGT TCA TCT GCA CCA C
	PMT-park-INS.rev	reverse	GGA CCA TGT GAT CGC TTC TC
pmTurquoise2-LC3	pmt-LC3-BB.for	forward	CCT GCT GGA GTT CGT GAC C
	pmt-LC3-BB.rev	reverse	GGT CAG CTT GCC GTA GGT G
	PMT-lc3-INS.for	forward	CTA CGG CAA GCT GAC CCT GA
	PMT-lc3-INS.rev	reverse	CAG GAA CTC CAG CAG GAC CA

Transcriptomic Analysis

Enrichment Analysis

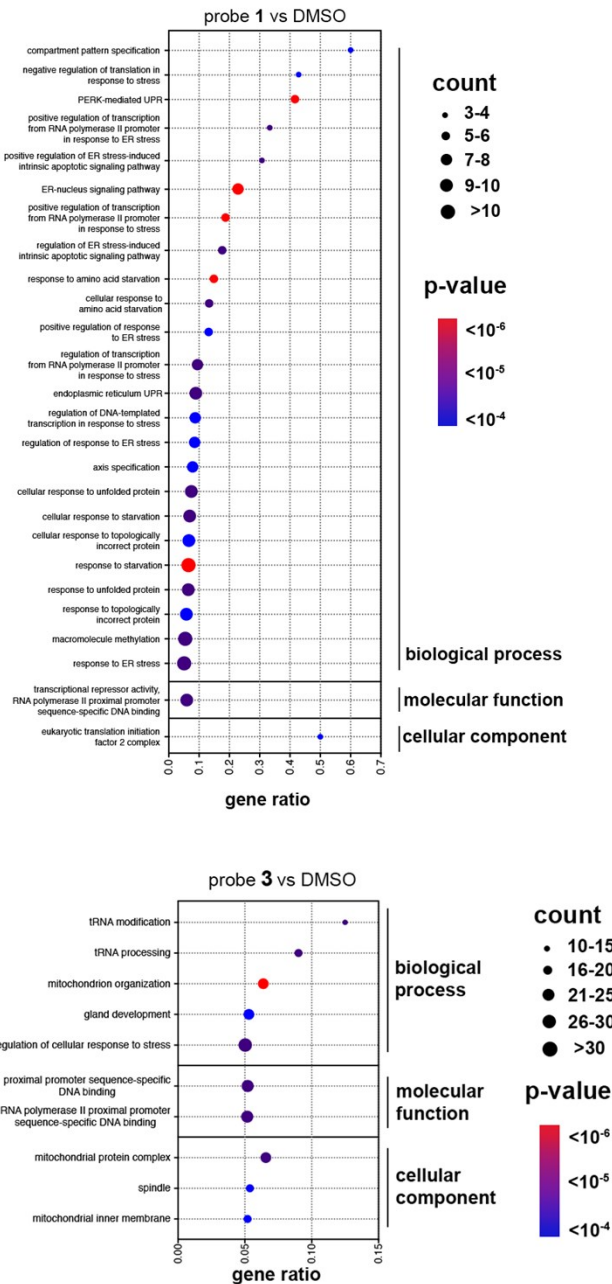


Figure S18. Enrichment analysis of significantly upregulated or downregulated genes in HEK293 cells using gene ontology (GO) database. **a**, Cells treated with probe 1 (15 μ M) compared to DMSO control. **b**, Cells treated with probe 3 (5 μ M) and compared to DMSO control. Size of circle represents the total number of genes associated with the function or cellular component. Gene ratio refers to the number of genes that are

differentially regulated divided by the total genes known to participate in a specific function or cellular component.

Adapter Sequences for RNA Sequencing

Oligonucleotide sequences for TruSeq™ RNA and DNA Sample Prep Kits

TruSeq Universal Adapter

5'-AATGATACGGCGACCACCGAGATCTACACTCTTTCCCTACACGACGCTCTTC
CGATCT

TruSeq™ Adapters

TruSeq Adapter, Index 1

5'-GATCGGAAGAGCACACGTCTGAACTCCAGTCACATCACGATCTCGTATGCC
GTCTTCTGCTTG

TruSeq Adapter, Index 2

5'-GATCGGAAGAGCACACGTCTGAACTCCAGTCACCGATGTATCTCGTATGCC
GTCTTCTGCTTG

TruSeq Adapter, Index 3

5'-GATCGGAAGAGCACACGTCTGAACTCCAGTCACTTAGGCATCTCGTATGCC
GTCTTCTGCTTG

TruSeq Adapter, Index 4

5'-GATCGGAAGAGCACACGTCTGAACTCCAGTCACTGACCAATCTCGTATGCC
GTCTTCTGCTTG

TruSeq Adapter, Index 5

5'-GATCGGAAGAGCACACGTCTGAACTCCAGTCACACAGTGATCTCGTATGCC
GTCTTCTGCTTG

TruSeq Adapter, Index 6

5'-GATCGGAAGAGCACACGTCTGAACTCCAGTCACGCCAATATCTCGTATGCC
GTCTTCTGCTTG

TruSeq Adapter, Index 7

5'-GATCGGAAGAGCACACGTCTGAACTCCAGTCACCAGATCATCTCGTATGCC
GTCTTCTGCTTG

TruSeq Adapter, Index 8

5'-GATCGGAAGAGCACACGTCTGAACTCCAGTCACACTTGAATCTCGTATGCCG
TCTTCTGCTTG

TruSeq Adapter, Index 9

5'-GATCGGAAGAGCACACGTCTGAACTCCAGTCACGATCAGATCTCGTATGCC
GTCTTCTGCTTG

TruSeq Adapter, Index 10

5'-GATCGGAAGAGCACACGTCTGAACTCCAGTCACTAGCTTATCTCGTATGCCG
TCTTCTGCTTG

TruSeq Adapter, Index 11

5'-GATCGGAAGAGCACACGTCTGAACTCCAGTCACGGCTACATCTCGTATGCC
GTCTTCTGCTTG

TruSeq Adapter, Index 12

5'-GATCGGAAGAGCACACGTCTGAACTCCAGTCACCTTGTAATCTCGTATGCCG
TCTTCTGCTTG

TruSeq Adapter, Index 13

5'-GATCGGAAGAGCACACGTCTGAACTCCAGTCACAGTCAACAATCTCGTATG
CCGTCTTCTGCTTG

TruSeq Adapter, Index 14

5'-GATCGGAAGAGCACACGTCTGAACTCCAGTCACAGTCCGTATCTCGTATG
CCGTCTTCTGCTTG

TruSeq Adapter, Index 15

5'-GATCGGAAGAGCACACGTCTGAACTCCAGTCACATGTCAGAATCTCGTATG
CCGTCTTCTGCTTG

TruSeq Adapter, Index 16

5'-GATCGGAAGAGCACACGTCTGAACTCCAGTCACCCGTCCCGATCTCGTATG
CCGTCTTCTGCTTG

TruSeq Adapter, Index 18 4

5'-GATCGGAAGAGCACACGTCTGAACTCCAGTCACGTCCGCACATCTCGTATG
CCGTCTTCTGCTTG

TruSeq Adapter, Index 19

5'-GATCGGAAGAGCACACGTCTGAACTCCAGTCACGTGAAACGATCTCGTATG
CCGTCTTCTGCTTG

TruSeq Adapter, Index 20

5'-GATCGGAAGAGCACACGTCTGAACTCCAGTCACGTGGCCTTATCTCGTATG
CCGTCTTCTGCTTG

TruSeq Adapter, Index 21

5'-GATCGGAAGAGCACACGTCTGAACTCCAGTCACGTTTCGGAATCTCGTATG
CCGTCTTCTGCTTG

TruSeq Adapter, Index 22

5'-GATCGGAAGAGCACACGTCTGAACTCCAGTCACCGTACGTAATCTCGTATG
CCGTCTTCTGCTTG

TruSeq Adapter, Index 23

5'-GATCGGAAGAGCACACGTCTGAACTCCAGTCACGAGTGGATATCTCGTATG
CCGTCTTCTGCTTG

TruSeq Adapter, Index 25

5'-GATCGGAAGAGCACACGTCTGAACTCCAGTCACACTGATATATCTCGTATGC
CGTCTTCTGCTTG

TruSeq Adapter, Index 27

5'-GATCGGAAGAGCACACGTCTGAACTCCAGTCACATTCCTTTATCTCGTATGC
CGTCTTCTGCTTG

Quantitative Image Analysis

Mitochondrial Morphologies

Mitochondrial morphology of live HEK293 cells was assessed by quantification of the signals obtained from activation of probe **1** or **3**. Cells were treated with probe **1** (15 μ M) or **3** (5 μ M) for 3-4 h. For the controls, CCCP (20 μ M, 2 h) or DMSO (3-4 h), mitochondria were stained with MitoTracker Deep Red (MDR). Good quality images, with strong signal but avoiding saturation, were collected in the red ($\lambda_{\text{ex}} = 561$ nm; $\lambda_{\text{em}} = 630 \pm 75$ nm) and far-red ($\lambda_{\text{ex}} = 640$ nm; $\lambda_{\text{em}} = 700 \pm 75$ nm) imaging channels. The images were collected using a 100 \times objective (100 \times 1.49 CFI Apo TIRF), an EMCCD camera (Digital Orca Flash 4.0 V2, rolling shutter usage, 1024 \times 1024 pixel (pixel size 13 μ m) with no binning (1 \times 1). Representative example of red images is displayed in Figure S19a. Binary images were generated by segmentation of red images. The following macro was applied in Fiji (ImageJ):

Binary macro

```
run("Subtract Background...", "rolling=50");
run("Despeckle");
run("Enhance Local Contrast (CLAHE)", "blocksize=9 histogram=256 maximum=4
mask=*None* fast_(less_accurate)");
run("Tubeness", "sigma=1.5");
setOption("BlackBackground", false);
run("Make Binary");
run("Invert");
```

Application of this macro generated binary images of mitochondria. Representative examples are displayed in Figure S19b. The shapes of mitochondria were analyzed using the “analyze particle” plugin from Fiji software. The scale was set and a centered region of interest of 800 \times 800 pixels was chosen to run the analysis, to avoid taking into account less intense signals on the edges of the frames. The following macro was applied in Fiji (ImageJ):

Scale macro

```
run("Set Scale...", "distance=100 known=13 pixel=1 unit=um");
run("Invert");
makeRectangle(112, 112, 800, 800);
run("Crop");
run("Set Measurements...", "area perimeter shape redirect=None decimal=5");
run("Analyze Particles...", "size=9-Infinity pixel show=Masks display
exclude");
```

The circularity, area and aspect ratio values for each mitochondrion were obtained from these measurements. Representative examples of obtained binary images are displayed in Figure S19c. The lengths of mitochondria were calculated using the scaled binary images and skeletonize plugin from Fiji. The skeletonize plugin thins mitochondria to be 1 pixel wide. The “analyze particle” plugin was used to determine the length of mitochondria, as the area of skeletonized mitochondria represent the total length of mitochondria in pixel. The following macro was applied in Fiji (ImageJ):

Skeletonize macro

```
run("Skeletonize (2D/3D)");
run("Analyze Particles...", "size=0-Infinity pixel show=Nothing display
exclude clear summarize");
```

Representative example of skeletonized image is displayed in Figure S19d. The length values for each mitochondrion were obtained from these measurements.

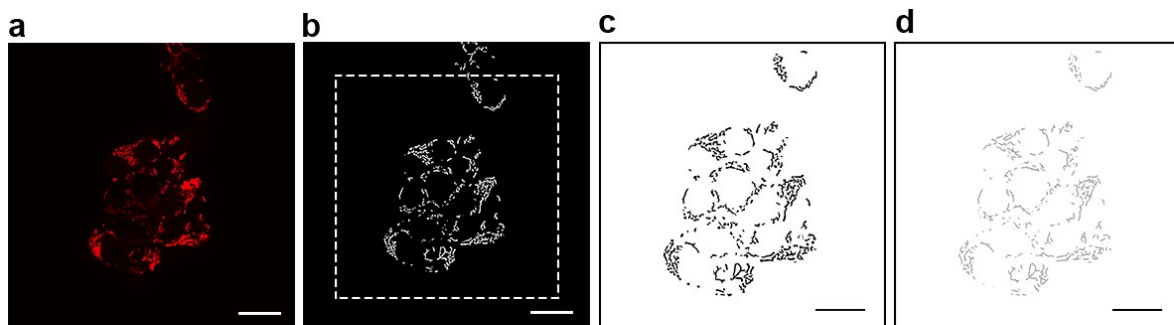


Figure S19. **a**, Example of red image of mitochondria. **b**, Segmented, binary image of mitochondria obtained employing “binary macro” on image a. **c**, Binary images were scaled and analyzed employing “scale macro” on image b. **d**, Binary image was skeletonized and analyzed employing “skeletonize macro” on image c. Scale bar = 20 μm .

Membrane Depolarization

Membrane depolarization of live HEK293 cells was assessed by quantification and localization of the signals obtained from activation of either probe **1** or **3** as well as CCCP stained with probe **3**. Cells were treated with **1** (15 μM), **3** (1 μM) or CCCP (20 μM) co-incubated with **3** for 2 h. Good quality images, with strong signal but avoiding saturation, were collected in the red ($\lambda_{\text{ex}} = 561 \text{ nm}$) imaging channel. The images were collected using a 60 \times objective (Silicon UPlanSApo 60 \times NA = 1.3), 4 GaAsP PMTs (spectral detection option) and a transmission PMT (800 \times 800 pixels, pixel size 7.5 μm). Representative example of red images is displayed in Figure S24a. A cell was chosen as region of interest. A pixel intensity threshold was set to differentiate the mitochondrial (Figure S20b) from the cytoplasmic fraction (Figure S20c). In a similar manner, a pixel intensity threshold was set to determine signal from noise (Fig. S20d). The following macros were applied in Fiji (ImageJ) after which the measure command was run:

mitochondrial macro

```
run("Duplicate...", " ");
run("Despeckle");
getRawStatistics(nPixels, mean, min, max);
    run("Find Maxima...", "noise="+max+" output=[Point Selection]");
getSelectionBounds(x, y, w, h);
print("coordinates=("+x+", "+y+")", value="+getPixel(x,y));
    run("Set Measurements...", "area mean min integrated limit
redirect=None decimal=5");
setThreshold(max*0.25, max);
```

cytoplasmic macro

```
run("Duplicate...", " ");
run("Despeckle");
getRawStatistics(nPixels, mean, min, max);
    run("Find Maxima...", "noise="+max+" output=[Point Selection]");
getSelectionBounds(x, y, w, h);
print("coordinates=("+x+", "+y+")", value="+getPixel(x,y));
```

```
run("Set Measurements...", "area mean min integrated limit
redirect=None decimal=5");
setThreshold(min*2, max*0.25);
```

noise macro

```
run("Duplicate...", " ");
run("Despeckle");
getRawStatistics(nPixels, mean, min, max);
run("Find Maxima...", "noise="+max+" output=[Point Selection]");
getSelectionBounds(x, y, w, h);
print("coordinates=("+x+", "+y+")", value="+getPixel(x,y));
run("Set Measurements...", "area mean min integrated limit
redirect=None decimal=5");
setThreshold(min, min*2);
```

Representative example of compartmentalized images is displayed in Figure S20. The intensities for each compartment were obtained from these measurements.

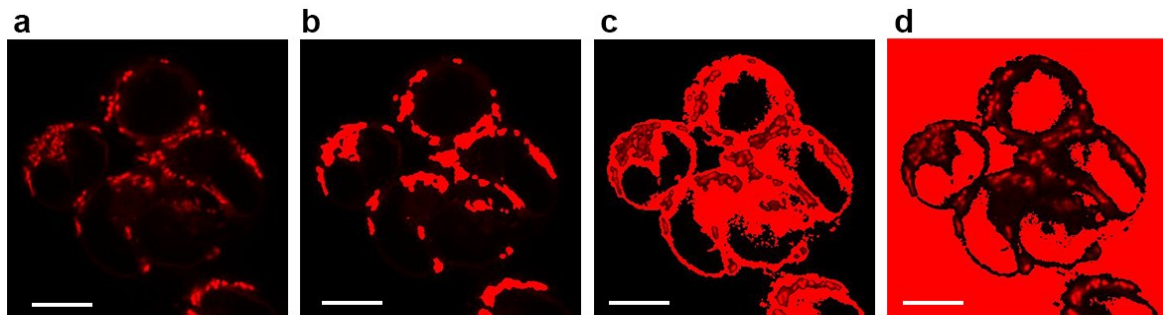


Figure S20. **a**, Example of red image of mitochondria. HEK293 cells were treated with probe **3** (1 μ M) for 2 h. **b**, Image of mitochondria fraction (red) obtained employing “mitochondrial macro” on image **a**. **c**, Image of cytoplasm (red) obtained employing “cytoplasm macro” on image **a**. **d**, Image of noise fraction obtained employing “noise macro” on image **a**. Scale bar = 10 μ m.

Co-localization of LC3 punctae and Mitochondria

Recruitment of LC3 to autophagosomes and mitochondria was assessed by quantification of the overlay of the signals of mTurquoise2-LC3 with the signals obtained from activation of either probe **1** or **3**. The cells were counterstained with Hoechst 33342 to identify the nuclei. Good quality images, with strong signal but avoiding saturation, were collected in the blue ($\lambda_{\text{ex}} = 405 \text{ nm}$; $\lambda_{\text{em}} = 450 \pm 50 \text{ nm}$), cyan

($\lambda_{\text{ex}} = 445 \text{ nm}$; $\lambda_{\text{em}} = 470 \pm 24 \text{ nm}$), and red ($\lambda_{\text{ex}} = 561 \text{ nm}$; $\lambda_{\text{em}} = 630 \pm 75 \text{ nm}$) imaging channels. The images were collected using a 100x objective (100x 1.49 CFI Apo TIRF), an EMCCD camera (Digital Orca Flash 4.0 V2, rolling shutter usage, 2048 x 2048 pixels, 6.5 x 6.5 μm) with no binning (1 x 1). Representative images are shown in Figure S21.

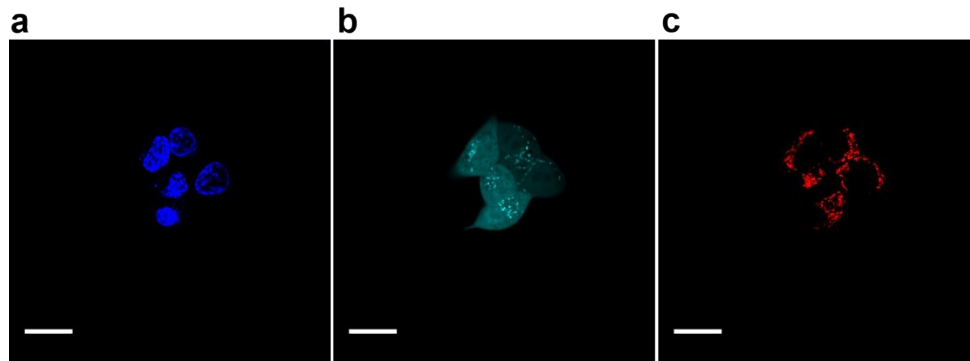


Figure S21. Representative images of **a**, Nuclei (blue channel); **b**, mTurquoise2-LC3 (cyan channel), and **c**, Mitochondria (red channel). Scale bar = 5 μm .

Binary images were generated by segmentation of the cyan and red images. For the cyan images, the following macro was applied in Fiji (ImageJ):

```
run("Duplicate...", "title=Original.tif");
run("Duplicate...", "title=Duplicate-1.tif");
run("Gaussian Blur...", "sigma=5");
imageCalculator("Subtract create", "Original.tif","Duplicate-1.tif");
close("Original.tif");
close("Duplicate-1.tif");
selectWindow("Result of Original.tif");
run("Duplicate...", "title=Duplicate-2.tif");
run("Gaussian Blur...", "sigma=5");
imageCalculator("Subtract create", "Result of Original.tif","Duplicate-2.tif");
close("Result of Original.tif");
close("Duplicate-2.tif");
selectWindow("Result of Result of Original.tif");
setAutoThreshold("MaxEntropy");
run("Make Binary");
run("Despeckle");
run("Invert");
run("Grays");
```

For the red images, the following macro was applied:

```
run("Subtract Background...", "rolling=50");  
run("Despeckle");  
run("Enhance Local Contrast (CLAHE)", "blocksize=9 histogram=256 maximum=4  
mask=*None* fast_(less_accurate)");  
run("Tubeness", "sigma=1.5");  
run("Make Binary");  
run("Grays");
```

Application of these macros generated binary images of LC3 vesicles and mitochondria. Representative examples are displayed in Figure S22.

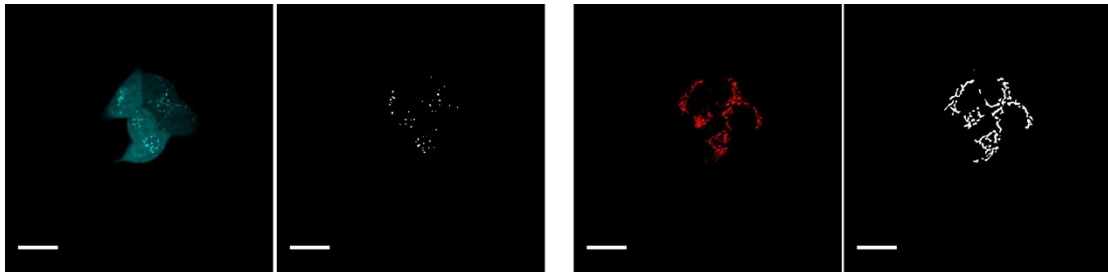


Figure S22. Examples of cyan and red images and their segmented, binary images obtained employing the macros described above. Scale bar = 5 μm .

The LC3 vesicles that co-localize with mitochondria were isolated by combining the two binary images in Fiji with the “Image calculator” and the “AND” function (Figure S23).

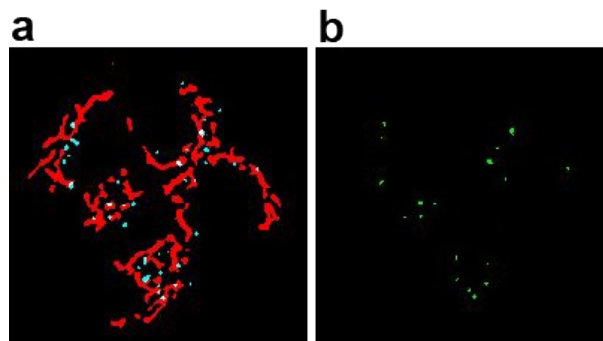


Figure S23. **a**, Overlay of mitochondria (red) and vesicles (cyan) binary images. **b**, Extracted vesicles that overlay with mitochondria using the AND function in Fiji.

The number of co-localized vesicles and mitochondria per cell was obtained using CellProfiler 3.0.0 (cellprofiler.org). Individual cells were identified as secondary objects of nuclei, which were identified as primary objects from raw blue channel images (Figure S24a,b). Cytosols were identified as secondary objects employing the identified nuclei and the image from the cyan channel, followed by masking to remove the area of the nuclei (Figure S24c,d). Finally, the extracted vesicles from the binary images (Figure S24b) were related to the identified cytosols and counted (Figure S24e). The CellProfiler pipeline file is available upon request.

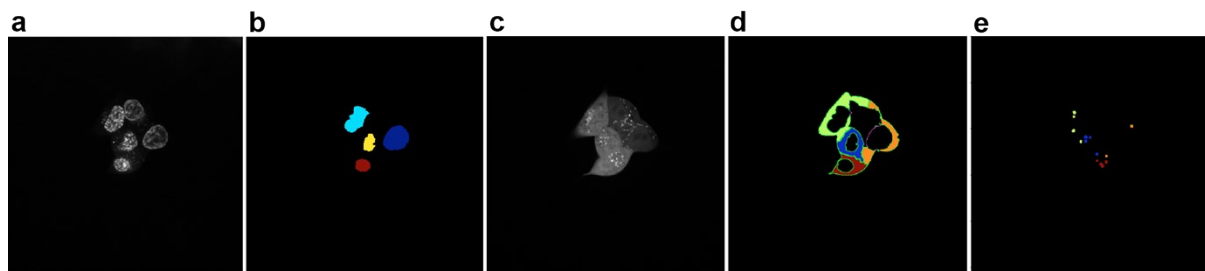
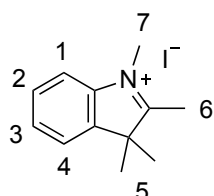


Figure S24. **a**, Raw image of nuclei. **b**, Segmentation of image a and identification of nuclei. **c**, Raw image of the cyan channel containing vesicles and cytosolic signals. **d**, Identification of cytosols as secondary objects based on the cyan image and the identified nuclei in image b. **e**, Identification of overlaid vesicles and mitochondria per cell.

Probe Characterization

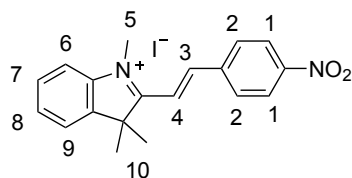
Synthesis of Probes

1,2,3,3-Tetramethyl-3*H*-indol-1-ium iodide (**5**)



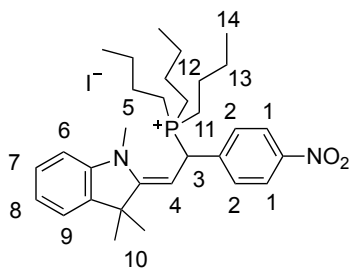
2,3,3-Trimethyl-3*H*-indole **2** (1.0 mL, 6.3 mmol) and iodomethane (0.5 mL, 7.5 mmol) were combined in a microwave vial and then sealed. The reaction mixture was heated at 120 °C in the microwave, set at very high absorbance for 20 min. The solid formed was washed with Et₂O to afford **5** as a pale yellow solid (1.26 g, 4.20 mmol, 67%). ¹H NMR (400 MHz, DMSO-*d*₆) δ = 7.91 (dd, *J* = 8.6, 2.4 Hz, 1H, H1), 7.82 (dd, *J* = 8.6, 2.4 Hz, 1H, H4), 7.66 – 7.59 (m, 2H, H2/3), 3.97 (s, 3H, H7), 2.76 (s, 3H, H6), 1.52 (s, 6H, H5) ppm. ¹³C NMR (101 MHz, DMSO-*d*₆) δ = 196.0, 142.1, 141.6, 129.3, 128.8, 123.3, 115.1, 53.9, 34.6, 21.7, 14.0 ppm. HRMS (ESI): exact mass calculated for [C₁₂H₁₆N]⁺: 174.1277; found: 174.1276.

(*E*)-1,3,3-Trimethyl-2-(4-nitrostyryl)-3*H*-indol-1-ium iodide (**3**)



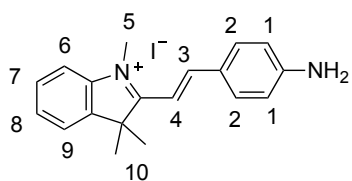
1,2,3,3-Tetramethyl-3*H*-indol-1-ium iodide **5** (50 mg, 0.17 mmol) and 4-nitrobenzaldehyde (25 mg, 0.17 mmol) were dissolved in EtOH (5 mL) and triethylamine (50 μL) was added to the solution. The reaction mixture was stirred at reflux for 18 h. The solvent was evaporated, the residue was dissolved in a minimum amount of CH₂Cl₂ and precipitated from Et₂O to afford **3** (27 mg, 0.06 mmol, 37%) as a red solid. *R*_f (SiO₂, CH₂Cl₂/MeOH 9:1) = 0.52. ¹H NMR (400 MHz, CD₃CN) δ = 8.41 – 8.35 (m, 2H, H2), 8.27 (d, *J* = 16.6 Hz, 1H, H3), 8.22 – 8.17 (m, 2H, H1), 7.80 – 7.74 (m, 2H, H6/7), 7.73 – 7.64 (m, 2H, H8/9), 7.57 (d, *J* = 16.6 Hz, 1H, H4), 4.12 (s, 3H, H5), 1.80 (s, 6H, H10) ppm. ¹³C NMR (101 MHz, CD₃CN) δ = 150.8, 140.8, 131.7, 131.6, 130.4, 125.2, 123.9, 117.5, 116.5, 47.5, 36.1, 25.5, 9.0 ppm. HRMS (ESI) calculated for [C₁₉H₁₉N₂O₂]⁺: 307.1441, found 307.1445.

(Z)-Tributyl(1-(4-nitrophenyl)-2-(1,3,3-trimethylindolin-2-ylidene)ethyl)phosphonium iodide (1)



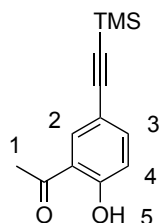
Compound **3** (13 mg, 0.03 mmol) was dissolved in dry CH_2Cl_2 (0.5 mL) in a Schlenk flask under inert atmosphere at room temperature. *n*-Tributyl phosphine (15 μL , 0.06 mmol) in CH_2Cl_2 (0.1 mL) was added dropwise to the stirring solution and an instant color change from orange to pale pink was observed. The crude product was purified by flash column chromatography (SiO_2 ; CH_2Cl_2 to $\text{CH}_2\text{Cl}_2/\text{CH}_3\text{OH}$ 98:2) to afford the nitro phosphonium **1** (17 mg, 0.026 mmol, 89%) as a yellow solid. ^1H NMR (300 MHz, CD_3CN) δ = 8.27 (dd, J = 8.2, 6.6 Hz, 2H, H2), 7.81 (dt, J = 8.6, 2.9 Hz, 2H, H1), 7.19 – 7.08 (m, 2H), 6.83 – 6.64 (m, 2H), 5.04 (dd, J = 16.8, 11.9 Hz, 1H), 4.64 (t, J = 11.5 Hz, 1H), 3.17 (s, 3H), 2.28 – 2.17 (m, PBU_3), 1.63 (s, 3H, H10), 1.44 (dt, J = 6.3, 3.5 Hz, PBU_3), 1.17 (s, 3H, H10), 0.90 (t, J = 7.2 Hz, PBU_3) ppm. ^{31}P NMR (122 MHz, CD_3CN) δ = 36.9, 35.8 ppm.

(E)-2-(4-Aminostyryl)-1,3,3-trimethyl-3H-indol-1-ium iodide (2)



1,2,3,3-Tetramethyl-3H-indol-1-ium iodide **5** (136 mg, 0.54 mmol) and 4-aminobenzaldehyde (65 mg, 0.54 mmol) were dissolved in EtOH (13 mL) and the reaction mixture was stirred at reflux for 5 h. The crude product was purified by flash column chromatography (SiO_2 ; CH_2Cl_2 to $\text{CH}_2\text{Cl}_2/\text{CH}_3\text{OH}$ 9:1) to afford **2** (148 mg, 0.37 mmol, 81%) as a red solid. R_f (SiO_2 , $\text{CH}_2\text{Cl}_2/\text{MeOH}$: 9/1) = 0.22. ^1H NMR (400 MHz, CD_3OD) δ = 8.27 (d, J = 15.6 Hz, 1H, H3), 7.84 (d, J = 8.7 Hz, 2H, H2), 7.67 – 7.49 (m, 4H, H6/7/8/9), 7.17 (d, J = 15.6 Hz, 1H, H4), 6.76 (d, J = 8.9 Hz, 2H, H1), 3.95 (s, 3H, H5), 1.80 (s, 6H, H10) ppm. HRMS (ESI) calculated for $[\text{C}_{19}\text{H}_{21}\text{N}_2]^+$: 277.1699, found 277.1701.

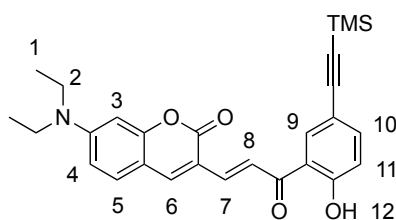
1-(2-Hydroxy-5-((trimethylsilyl)ethynyl)phenyl)ethan-1-one (6)



1-(5-Bromo-2-hydroxyphenyl)ethan-1-one (400 mg, 1.9 mmol) was dissolved in dry NEt_3 (8 mL) under inert atmosphere and the solution was stirred for 5 min at room temperature. $\text{PdCl}_2(\text{PPh}_3)_2$ (42 mg, 0.06 mmol) and CuI (14 mg, 0.07 mmol) were added and the solution was

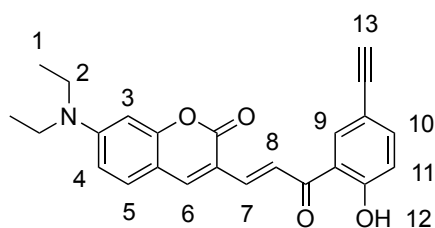
degassed. Ethynyltrimethylsilane (0.4 mL, 2.8 mmol) was added and the mixture was heated at 80 °C for 3 hours. The mixture was slowly cooled to room temperature, dry THF (10 mL) was added and stirred at room temperature for 1 h. The solvent was evaporated under reduced pressure, and the concentrate was diluted with CH₂Cl₂ and washed with water. The aqueous phase was extracted with CH₂Cl₂, the organic layers were combined and dried over anhydrous Na₂SO₄. The solvent was evaporated and the remaining oil was purified by flash chromatography (SiO₂; hexane/EtOAc 9:1 to 7:3) to yield 1-(2-hydroxy-5-((trimethylsilyl)ethynyl)phenyl)ethan-1-one as a pale yellow oil (349 mg, 1.5 mmol, 80%). ¹H NMR (400 MHz, CDCl₃) δ = 12.37 (s, 1H, H5), 7.86 (d, *J* = 2.1 Hz, 1H, H2), 7.55 (dd, *J* = 8.6, 2.1 Hz, 1H, H3), 6.91 (d, *J* = 8.6 Hz, 1H, H4), 2.64 (s, 3H, H1), 0.25 (s, 9H, TMS) ppm. ¹³C NMR (101 MHz, CDCl₃) δ = 204.3, 162.6, 139.8, 134.2, 119.5, 118.9, 114.1, 104.0, 26.9, 0.1 ppm.

(*E*)-7-(Diethylamino)-3-(3-(2-hydroxy-5-((trimethylsilyl)ethynyl)phenyl)-3-oxoprop-1-en-1-yl)-2*H*-chromen-2-one (7)



Compound **6** (176 mg, 0.76 mmol) and 7-(diethylamino)-2-oxo-2*H*-chromene-3-carbaldehyde (104 mg, 0.42 mmol) were dissolved in 3.2 mL of CH₂Cl₂/EtOH (1:1, v/v) and 2 drops of pyrrolidine were added. The resulting clear red solution was stirred at room temperature for 16 h. The solvent was evaporated under reduced pressure to afford a pale red solid that was purified by gradient flash chromatography (SiO₂; hexane/EtOAc 9:1 to 7:3) to yield the desired product **7** as a red solid (80 mg, 0.17 mmol, 41%). ¹H NMR (400 MHz, CDCl₃) δ = 13.22 (s, 1H, H12), 8.29 (d, *J* = 15.0 Hz, 1H, H7), 8.13 (d, *J* = 2.0 Hz, 1H, H3), 7.83 (s, 1H, H6), 7.73 (d, *J* = 15.0 Hz, 1H, H8), 7.55 (dd, *J* = 8.6, 2.0 Hz, 1H, H4), 7.36 (d, *J* = 8.9 Hz, 1H, H11), 6.93 (d, *J* = 8.6 Hz, 1H, H5), 6.64 (dd, *J* = 8.9, 2.5 Hz, 1H, H10), 6.52 (d, *J* = 2.5 Hz, 1H, H9), 3.47 (q, *J* = 7.2 Hz, 6H, H2), 1.26 (t, *J* = 7.1 Hz, 9H, H1), 0.27 (s, 9H, TMS) ppm.

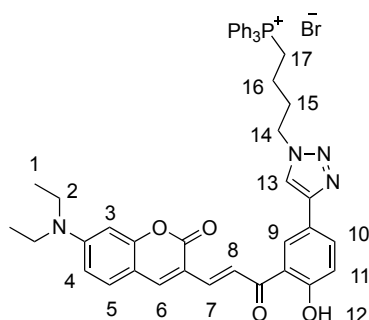
(*E*)-7-(Diethylamino)-3-(3-(5-ethynyl-2-hydroxyphenyl)-3-oxoprop-1-en-1-yl)-2*H*-chromen-2-one (8)



Compound **7** (50 mg, 0.11 mmol) was dissolved in dry THF (1.5 mL) and a solution of TBAF in dry THF (0.22 mL, 1 M) was added dropwise. The reaction mixture was stirred at room temperature for 30 min, and water (2 mL) was added. The mixture was

extracted twice with EtOAc, the organic layers were combined and dried over anhydrous Na₂SO₄, filtered and concentrated under reduced pressure. Purification was performed by flash chromatography (SiO₂; hexane/EtOAc 9:1 to 1:1). Compound **8** was isolated as a red solid (37 mg, 0.1 mmol, 87%). ¹H NMR (400 MHz, CDCl₃) δ = 13.23 (s, 1H, H12), 8.29 (d, *J* = 15.0 Hz, 1H, H7), 8.17 (d, *J* = 2.0 Hz, 1H, H3), 7.83 (s, 1H, H6), 7.74 (d, *J* = 15.0 Hz, 1H, H8), 7.57 (dd, *J* = 8.6, 2.0 Hz, 1H, H4), 7.35 (d, *J* = 8.9 Hz, 1H, H11), 6.96 (d, *J* = 8.6 Hz, 1H, H5), 6.64 (dd, *J* = 8.9, 2.5 Hz, 1H, H10), 6.53 (d, *J* = 2.4 Hz, 1H, H9), 3.47 (q, *J* = 7.1 Hz, 6H, H2), 3.03 (s, 1H, H12), 1.25 (t, *J* = 7.1 Hz, 9H, H1) ppm. ¹³C NMR (101 MHz, CDCl₃) δ = 194.0, 164.0, 160.2, 157.0, 152.4, 147.3, 141.7, 139.5, 134.3, 130.5, 120.9, 120.2, 118.9, 114.7, 112.8, 110.0, 109.2, 97.2, 83.0, 45.3, 12.6. ppm

(*E*)-(4-(4-(3-(3-(7-(Diethylamino)-2-oxo-2*H*-chromen-3-yl)acryloyl)-4-hydroxyphenyl)-1*H*-1,2,3-triazol-1-yl)butyl)triphenylphosphonium bromide (9**)**

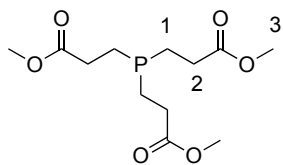


Compound **8** (10 mg, 0.09 mmol) and (4-azidobutyl)triphenylphosphonium bromide (12 mg, 0.09 mmol) were dissolved in degassed CH₂Cl₂ (1 mL) and bis(triphenylphosphine)copper(I) nitrate was added.

The mixture was stirred at room temperature for 1.5 h NEt₃ (2 drops) was added. The mixture was stirred for an additional 1 h. The mixture was diluted in CH₂Cl₂ and washed with water. The organic layer was dried over Na₂SO₄, filtered and concentrated under reduced pressure. Purification was performed by flash chromatography (SiO₂; CH₂Cl₂ to CH₂Cl₂/MeOH 9:1). Compound **9** was obtained as a red solid (12 mg, 0.05 mmol, 60%). ¹H NMR (400 MHz, CDCl₃) δ = 13.31 (s, 1H, H12), 8.77 (m, 1H, H7), 8.47 (s, 2H, H3/6), 8.19 – 7.98 (m, 3H, H8/4/11), 7.73 – 7.47 (m, 16H, H13/(Ph)₃), 7.06 (d, *J* = 6.8 Hz, 1H, H5), 6.59 (m, 1H, H10), 6.44 (s, 1H, H9), 4.63 (m, 2H, H14), 3.41 (q, *J* = 7.1 Hz, 4H, H2), 2.41 (m, 2H, H15), 2.00 (m, 2H, H17), 1.57 (m, 2H, H16), 1.21 (t, *J* = 7.1 Hz, 6H, H1)

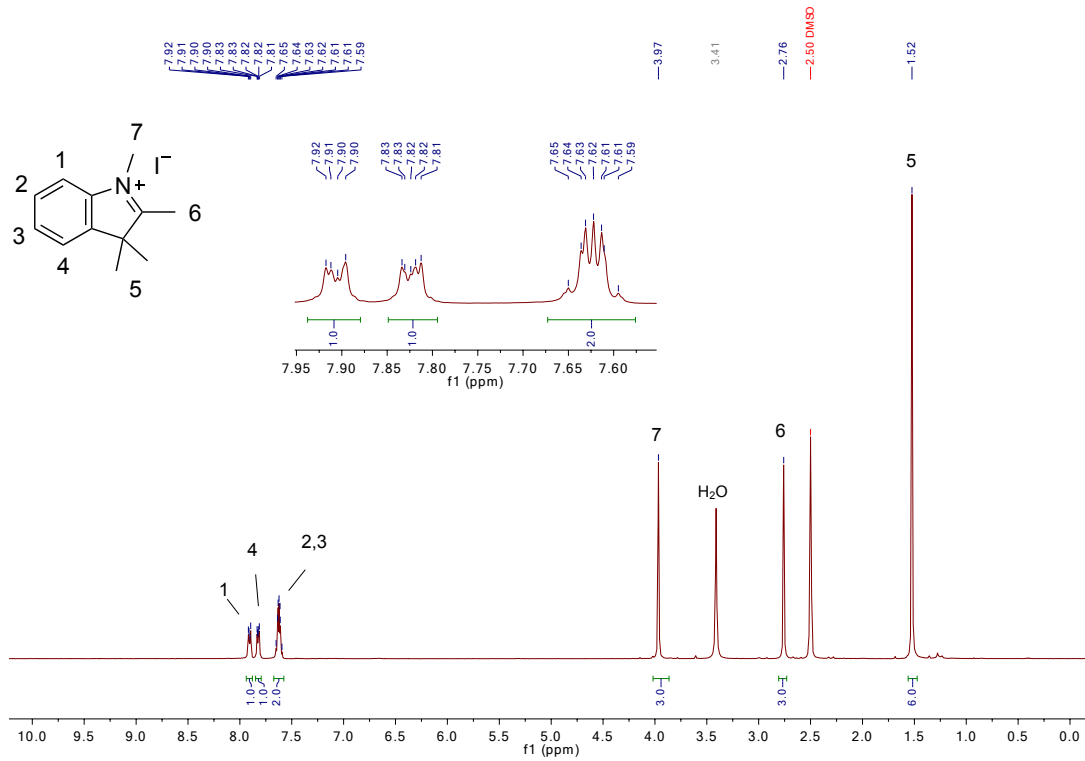
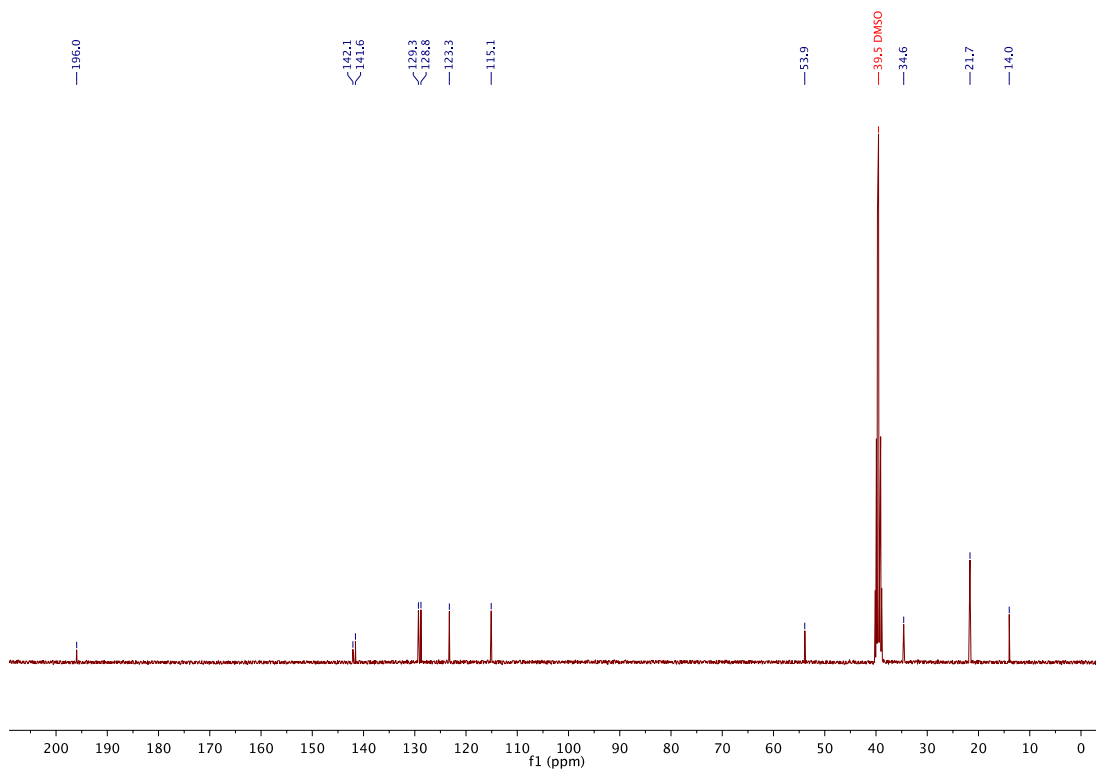
ppm. HRMS (TOF MS ES+) calculated for $[C_{46}H_{44}N_4O_4P]^+$: 747.3095, found: 747.3112.

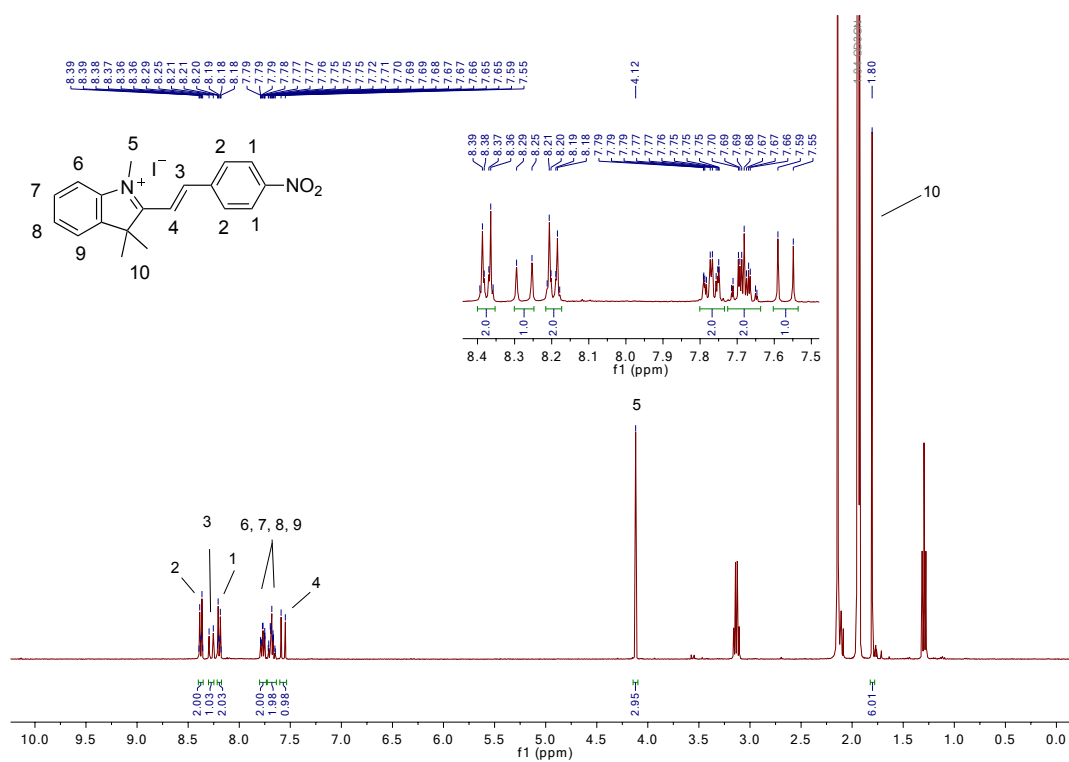
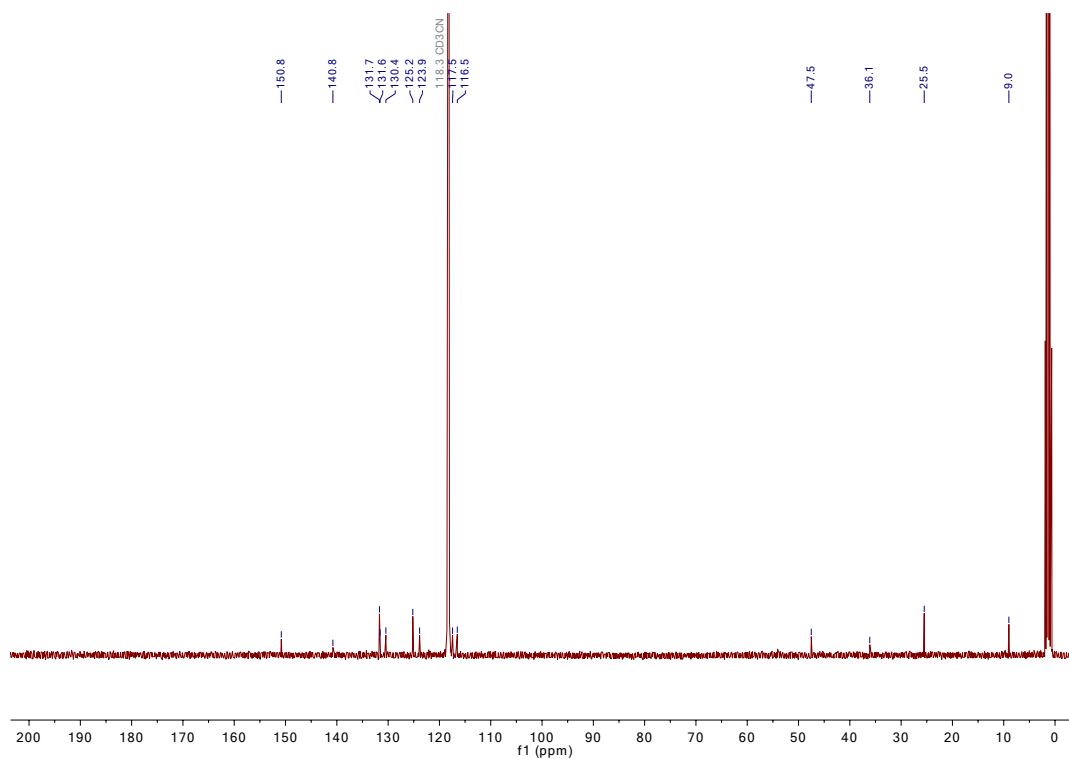
Trimethyl 3,3',3''-phosphanetriyltripropionate (tmTCEP)

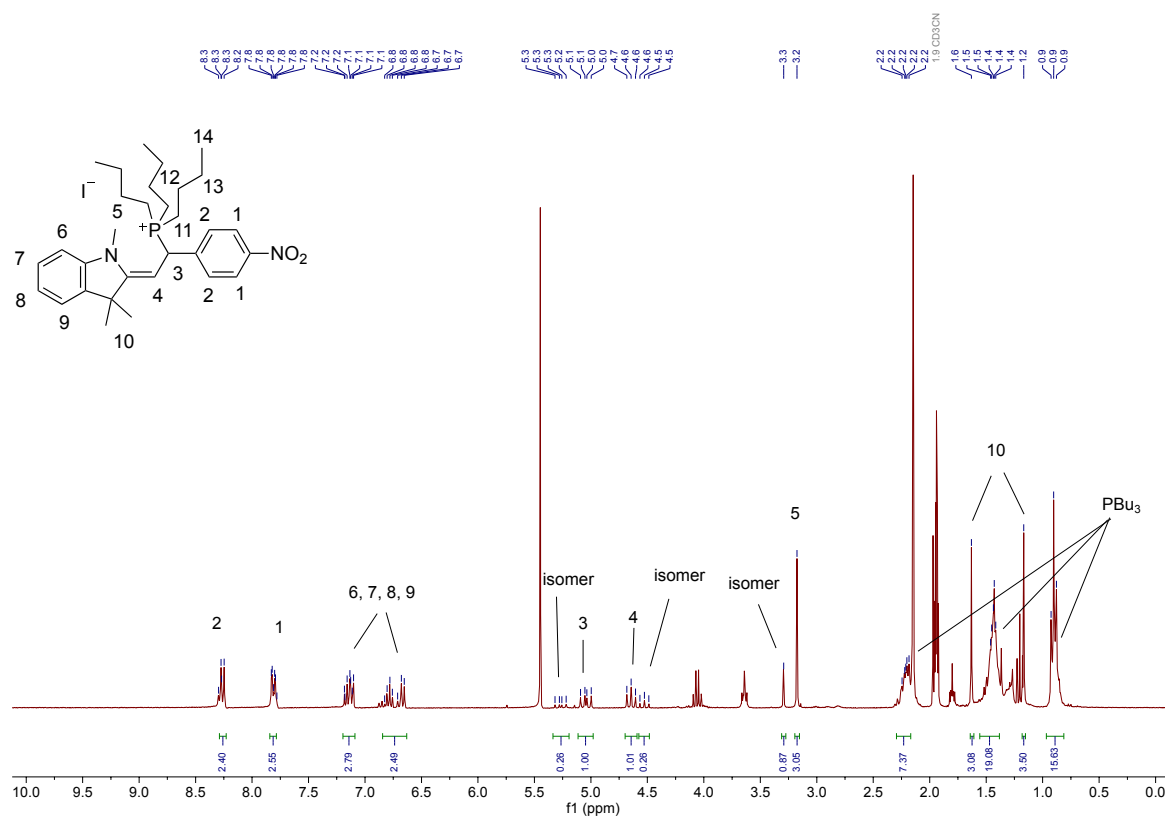
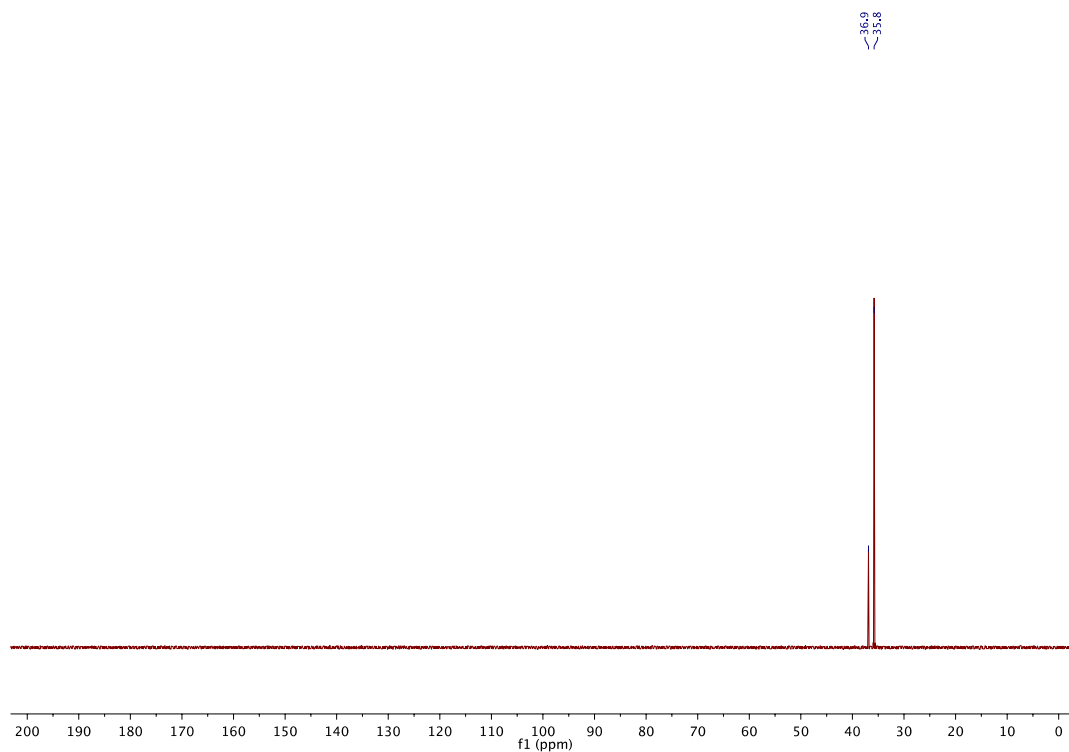


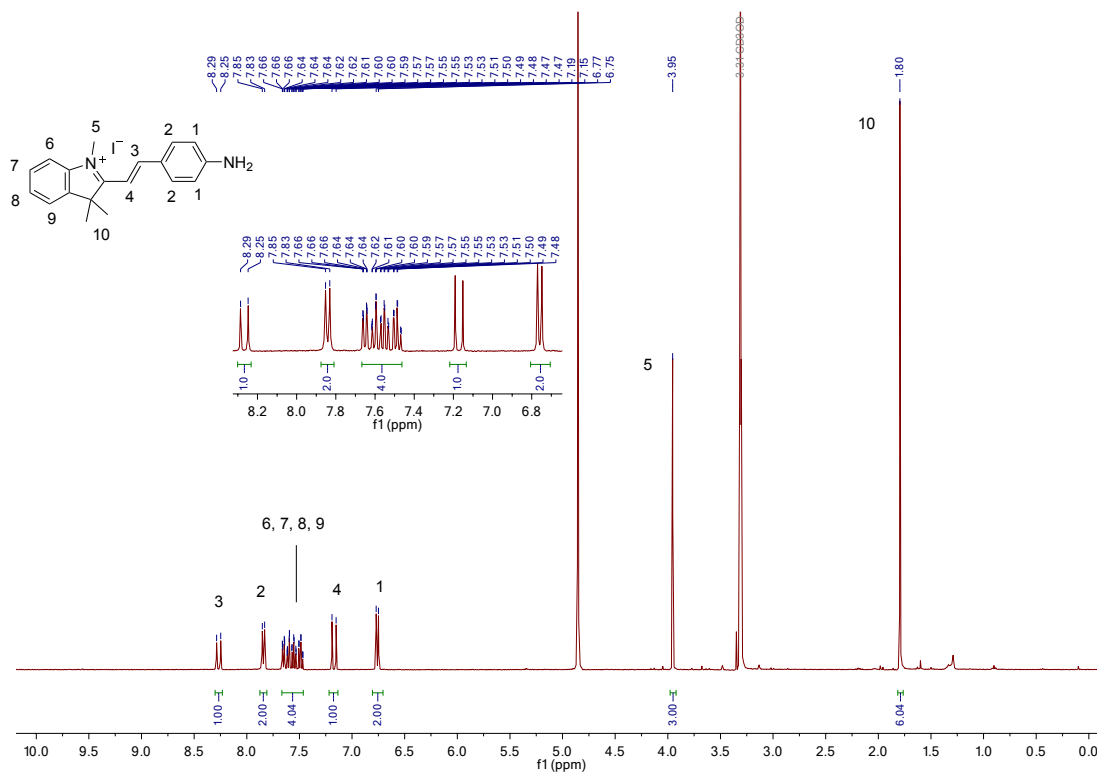
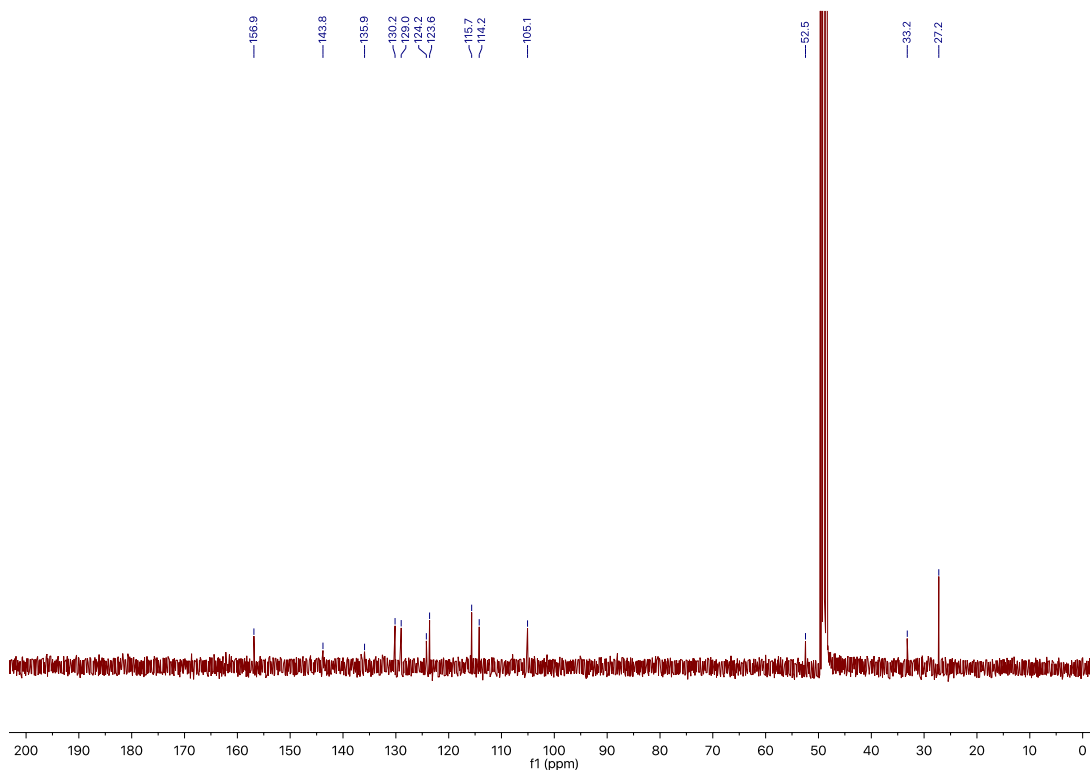
TCEP HCl (100 mg, 0.35 mmol) and Amberlyst 15 hydrogen form (dry, 100 mg) were combined in MeOH (dry, 4 mL). The reaction mixture was stirred at room temperature for 3 h under an inert atmosphere. The progress of the reaction was followed by TLC and LC-MS. Amberlyst was removed by filtration and the solvent was evaporated under reduced pressure. The crude product was purified by reversed-phase chromatography using a 4 g C18 column: gradient 5%-70% CH₃CN in H₂O / CH₃CN + 0.1% TFA) yielding tmTCEP as a clear, colorless oil (20 mg, 20%). ¹H NMR (400 MHz, CDCl₃) δ = 3.75 (s, 9H, H3), 2.93 (dt, J = 20.8, 6.6 Hz, 6H, H1), 2.58 (dt, J = 12.9, 6.3 Hz, 6H, H2) ppm. ¹³C NMR (101 MHz, CDCl₃) δ = 173.7 (d, J = 4.3 Hz), 53.0, 28.4 (d, J = 6.2 Hz), 17.2 (d, J = 52.0 Hz) ppm. ³¹P NMR (162 MHz, CDCl₃) δ = 20.5 ppm. HRMS (TOF MS ES+) calculated for $[C_{12}H_{22}O_6P]^+$: 293.1149, found: 293.1152.

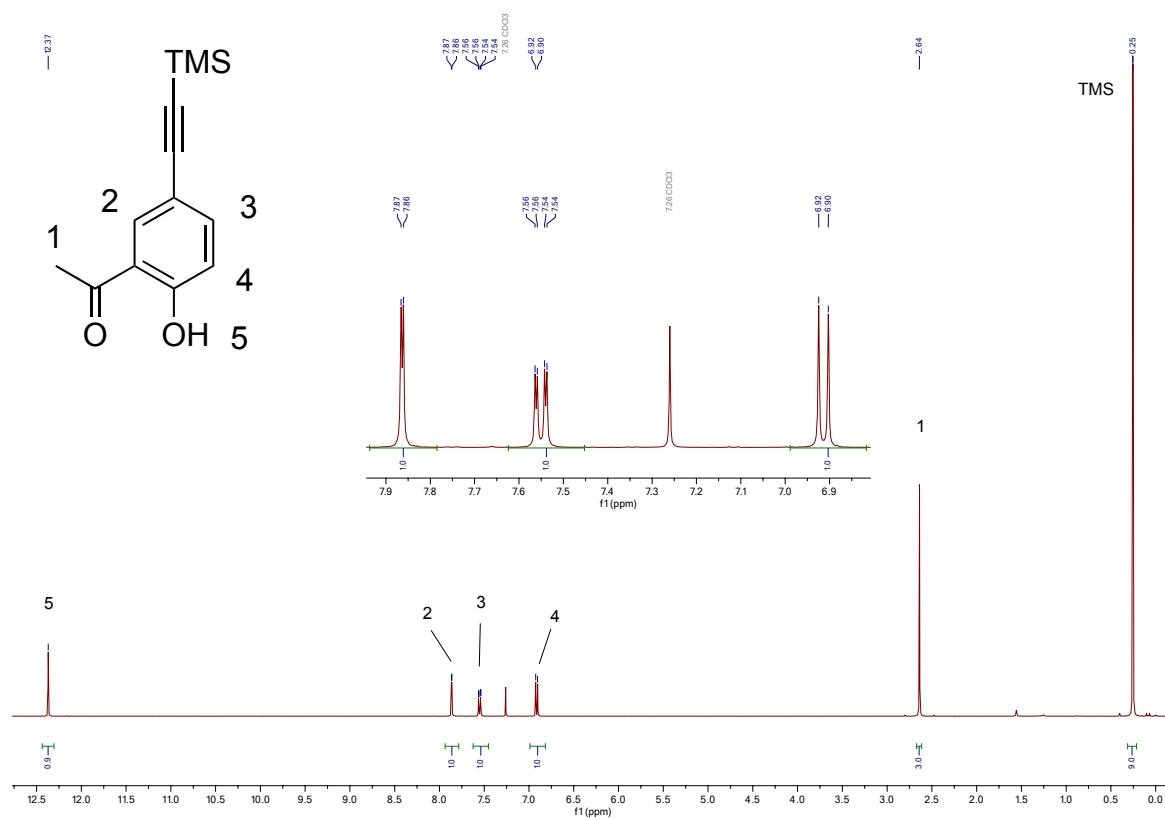
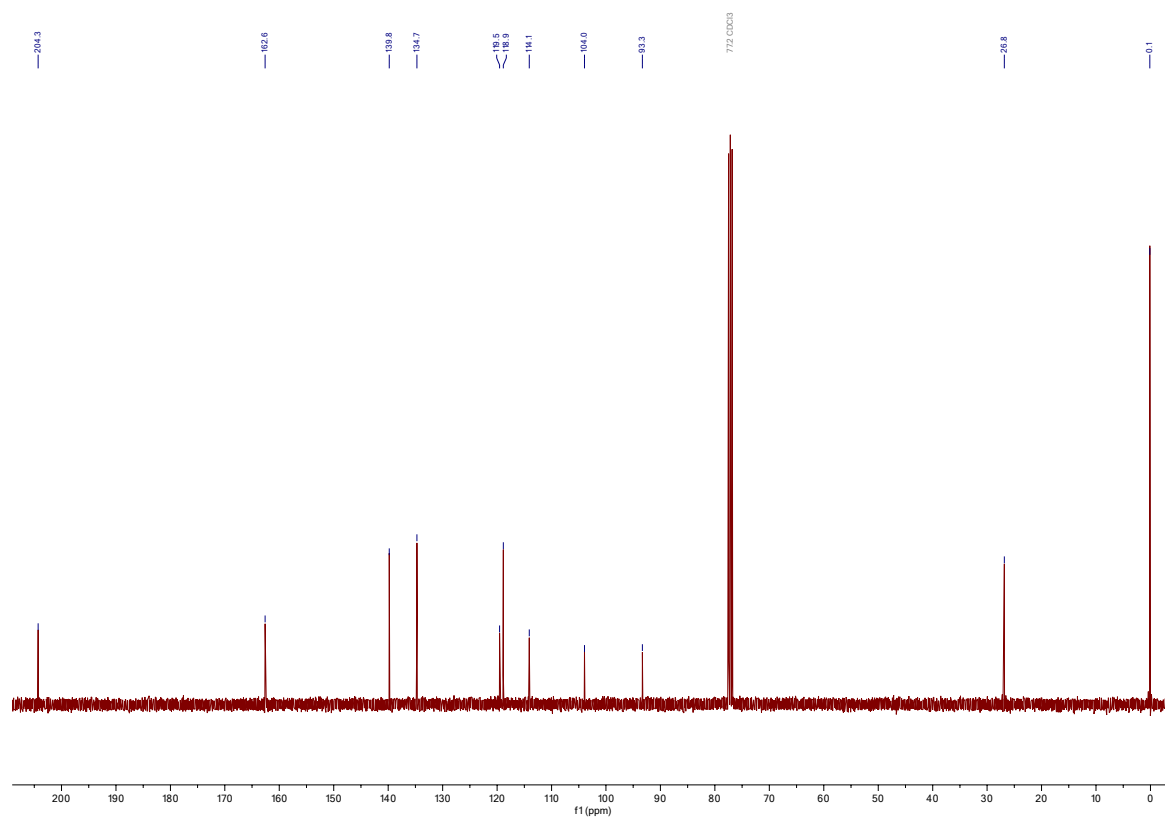
NMR Spectra

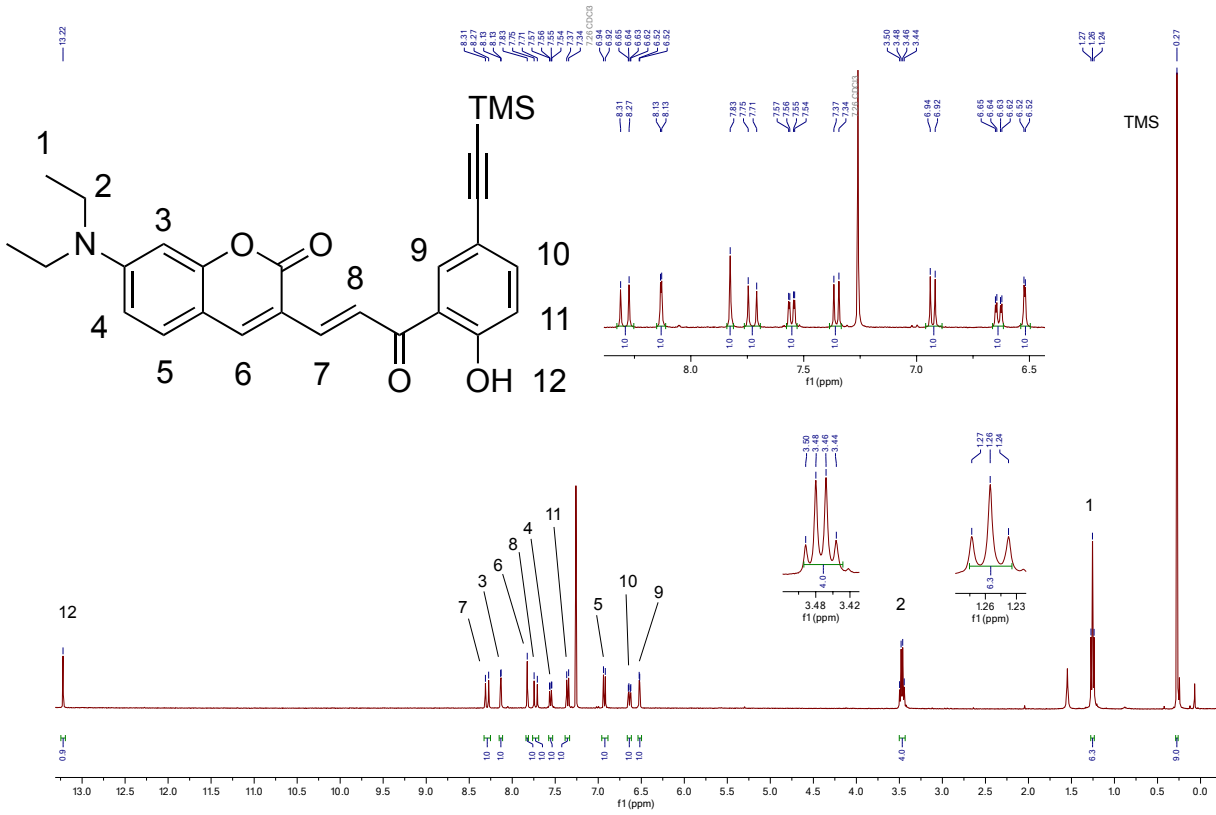
 ^1H NMR (400 MHz, $\text{DMSO-}d_6$) spectrum of **5** ^{13}C NMR (101 MHz, $\text{DMSO-}d_6$) spectrum of **5**

^1H NMR (400 MHz, $\text{CD}_3\text{CN}-d_3$) spectrum of **3** ^{13}C NMR (101 MHz, $\text{CD}_3\text{CN}-d_3$) spectrum of **3**

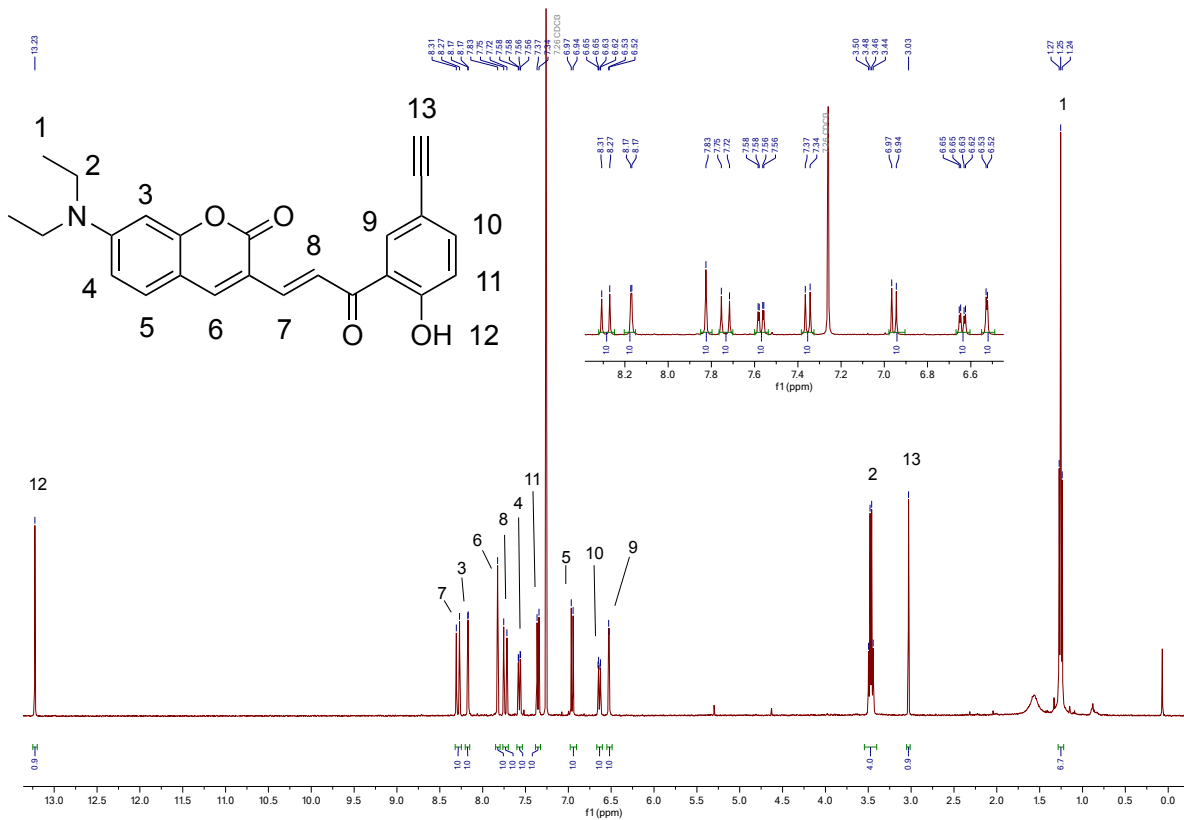
^1H NMR (300 MHz, $\text{CD}_3\text{CN}-d_3$) spectrum of **1** ^{31}P NMR (122 MHz, $\text{CD}_3\text{CN}-d_3$) spectrum of **1**

^1H NMR (400 MHz, $\text{CD}_3\text{OD}-d_4$) spectrum of **2** ^{13}C NMR (101 MHz, $\text{CD}_3\text{OD}-d_4$) spectrum of **2**

^1H NMR (400 MHz, CDCl_3 -*d*) spectrum of **6** ^{13}C NMR (101 MHz, CDCl_3 -*d*) spectrum of **6** ^1H NMR (400 MHz, CDCl_3 -*d*) spectrum of **7**

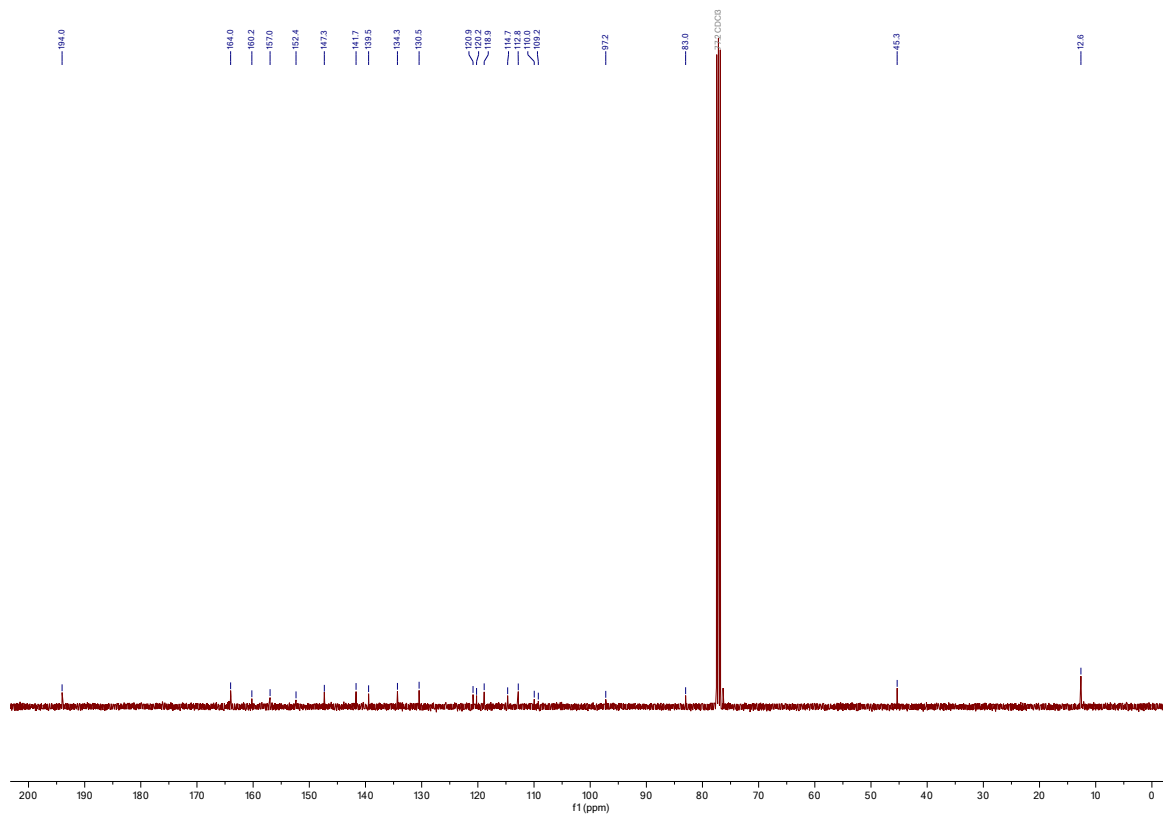


¹H NMR (400 MHz, CDCl₃-d) spectrum of 8

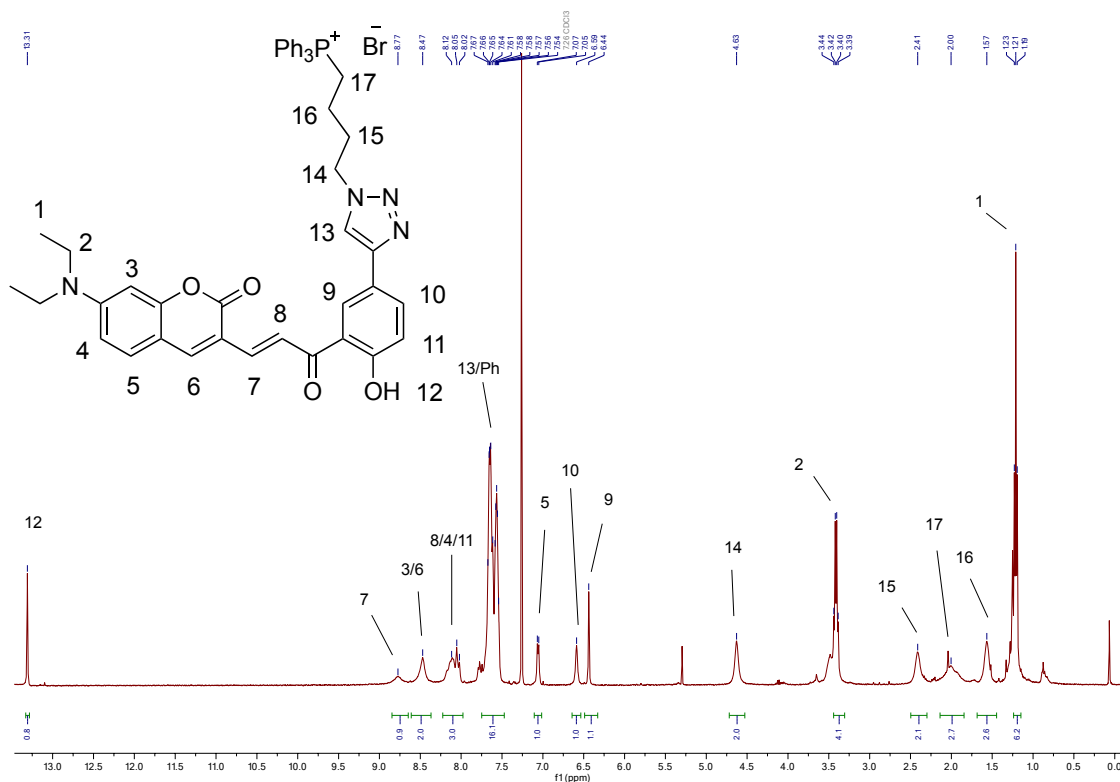


¹³C NMR (101 MHz, CDCl₃-d) spectrum of 8

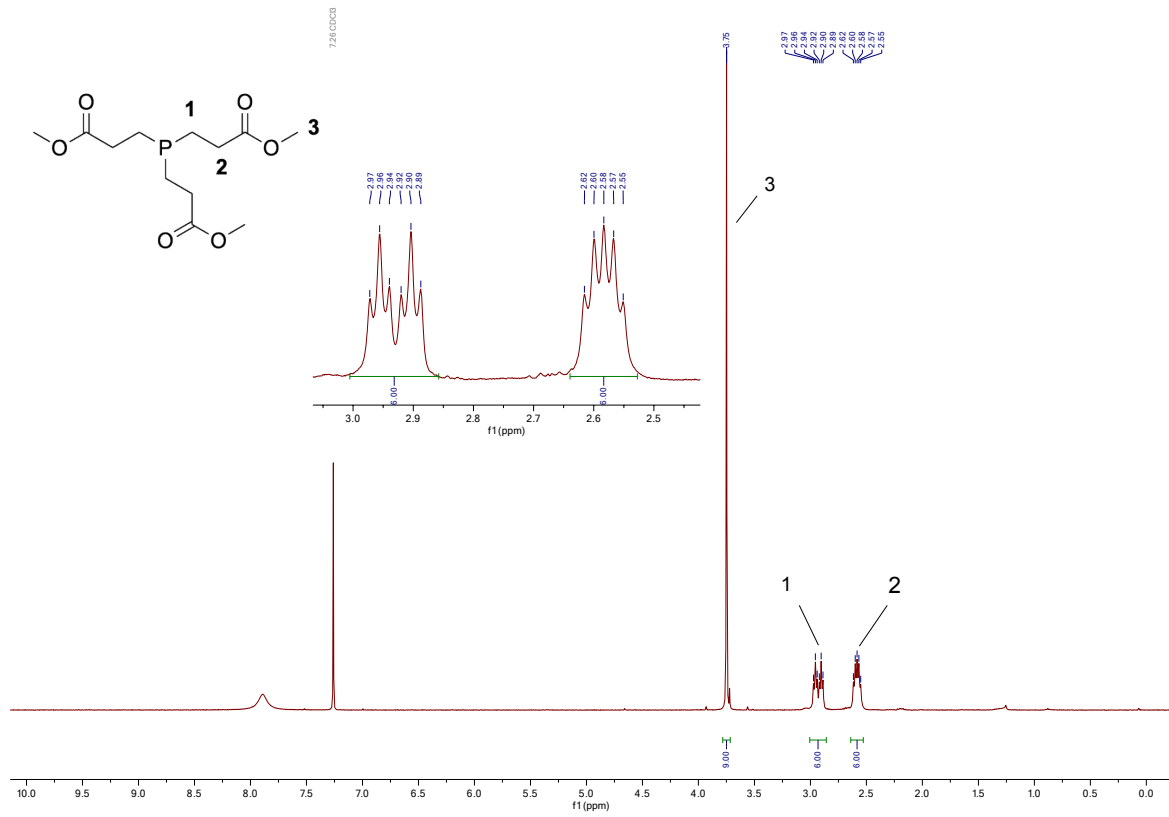
SI-50



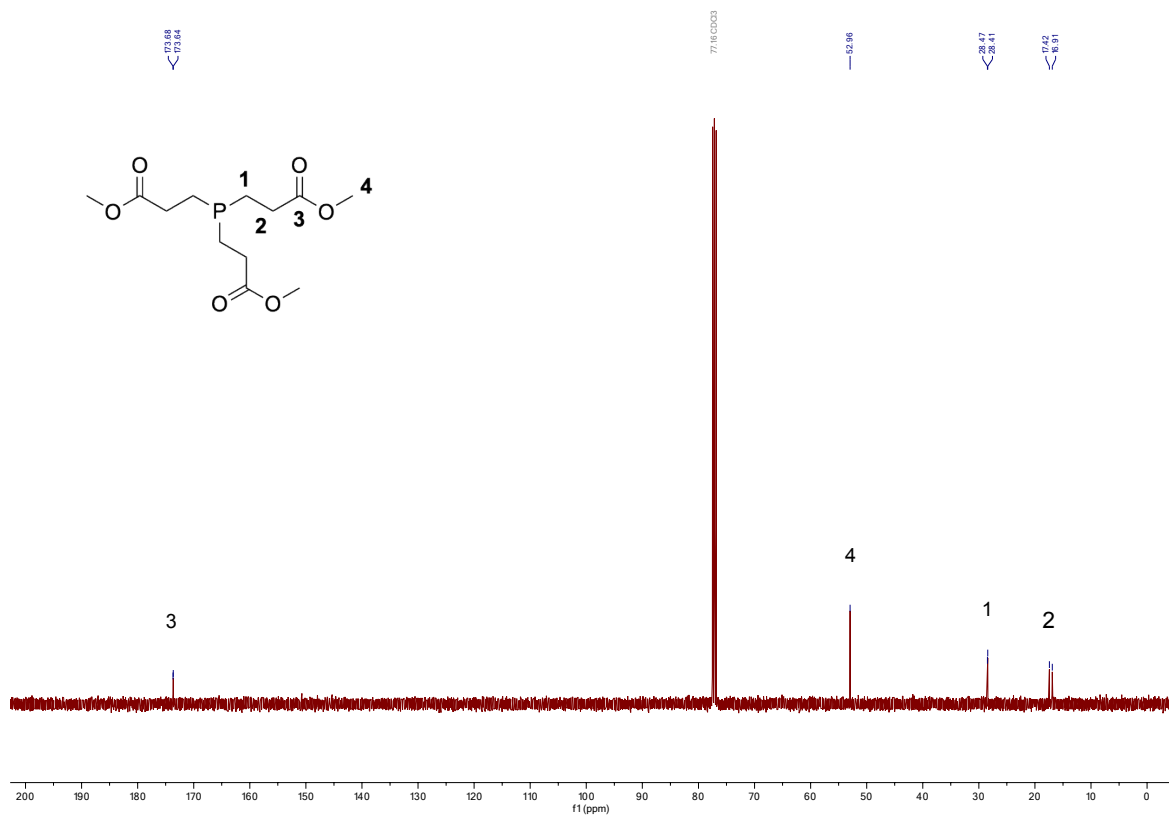
¹H NMR (400 MHz, CDCl₃-d) spectrum of **9**



¹H NMR (400 MHz, CDCl₃-d) spectrum of **tmTCEP**



¹³C NMR (101 MHz, CDCl₃-d) spectrum of **tmTCEP**



Bibliography

- [1] D. G. Gibson, L. Young, R.-Y. Chuang, J. C. Venter, C. A. Hutchison, H. O. Smith, *Nat. Methods* **2009**, *6*, 343–345.
- [2] E. A. Halabi, D. Pinotsi, P. Rivera-Fuentes, *Nat. Commun.* **2019**, *10*, 1232.
- [3] J. Goedhart, D. von Stetten, M. Noirclerc-Savoye, M. Lelimosin, L. Joosen, M. A. Hink, L. van Weeren, T. W. J. Gadella Jr, A. Royant, *Nat. Commun.* **2012**, *3*, 751.
- [4] M. Shaofei Zhang, S. F. Brunner, N. Huguenin-Dezot, A. Deliz Liang, W. H. Schmied, D. T. Rogerson, J. W. Chin, *Nat. Methods* **2017**, *14*, 729–736.
- [5] A. M. Bolger, M. Lohse, B. Usadel, *Bioinformatics* **2014**, *30*, 2114–2120.
- [6] A. Dobin, C. A. Davis, F. Schlesinger, J. Drenkow, C. Zaleski, S. Jha, P. Batut, M. Chaisson, T. R. Gingeras, *Bioinformatics* **2013**, *29*, 15–21.
- [7] M. Lawrence, W. Huber, P. Hervé, P. Aboyoun, M. Carlson, R. Gentleman, M. T. Morgan, V. J. Carey, *PLOS Comput. Biol.* **2013**, *9*, e1003118.
- [8] M. D. Robinson, D. J. McCarthy, G. K. Smyth, *Bioinformatics* **2010**, *26*, 139–140.